Gas-Phase Transition-Metal Negative Ion Chemistry

ROBERT R. SQUIRES

Department of Chemistry, Purdue University, West Lafayette, Indiana 47907

Received January 21, 1987

Contents

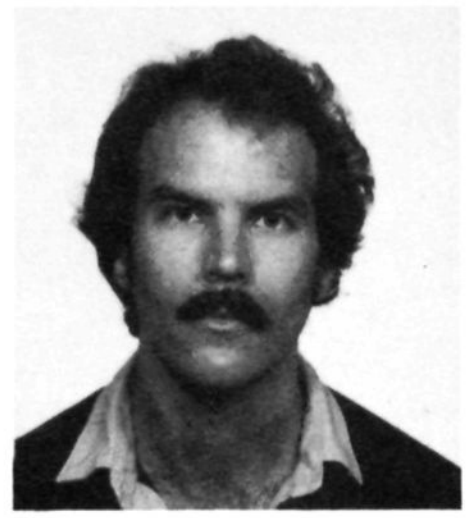

Robert R. Squires was born in Oakland, CA, in 1953. He received the Ph.D. degree from Yale University in 1980 for work with K. B. Wiberg on steric effects and reaction calorimetry. He spent a brief period as a postdoctoral research associate with C. H. DePuy and V. M. Bierbaum at the University of Colorado and moved to Purdue University as assistant professor in 1981. He was promoted to associate professor in 1986 and is currently a Fellow of the Alfred P. Sloan Foundation. His research centers on the flowing afterglow–triple quadrupole technique and its use in the study of gas-phase organic and organometallic ion chemistry.

I. Introduction

One of the most active new growth areas in mass spectrometry and gas-phase ion chemistry involves the study of ion–molecule reactions of transition-metal complexes and the chemistry of gaseous atomic metal ions. The number of publications concerning gas-phase metal ion chemistry and the number of research groups working in this area have increased steadily, especially in the past dozen years or so.[1] It is no accident that this activity coincides with the explosive growth of organometallic chemistry in recent years, for it is the same richness and diversity in the behavior of transition-metal compounds that have attracted the interests of gas-phase ion chemists. As a direct result of gas-phase metal ion studies, valuable new thermochemical data for inorganic and organometallic compounds have become available such as homolytic and heterolytic metal–ligand bond strengths.[2] With the use of a variety of experimental techniques, gas-phase ion chemists have been able to generate and directly examine many of the otherwise elusive reactive intermediate species postulated for condensed-phase organometallic reactions, and to affect the "synthesis" and study of novel metal ion complexes exhibiting rare types of bonding and/or unusual properties. From an analytical perspective, gas-phase metal ion chemistry has been an obvious boon to inorganic and organometallic mass spectrometry, and gaseous metal ions have also shown potential for use in chemical ionization mass spectrometry.[3]

While the situation has improved somewhat in recent years, negative ions have traditionally been the "orphaned children" of mass spectrometry, accounting for a relatively small portion of the literature compared to their positive-ion siblings.[4] This has been especially true of gas-phase metal ion chemistry, despite the important stature negative ions enjoy in inorganic and organometallic chemistry in solution. For example, anionic metal complexes and nucleophilic addition mechanisms involving anionic reagents and metal substrates play important roles in a variety of industrially important processes such as Reppe reactions, Wacker oxidations, and numerous homogeneous models for Fischer–Tropsch and water gas shift cycles.[5] Moreover, new methods for transition-metal-mediated organic synthesis frequently employ metal anion intermediates and reactions of anionic nucleophiles with metal-coordinated organic ligands.[6] The properties and reactivity of multiply-charged organometallic negative ions have also attracted much attention recently as a novel class of potentially powerful reducing agents.[7] Thus, the relative neglect of negative ions in gas-phase metal ion chemistry by no means reflects a lack of pertinence. Rather, it is undoubtedly due to the relative ease with which positive metal ions and metal ion complexes can be made in the gas phase and, as will become clear from this review, their generally greater reactivity compared to that of negative ions.

This review will present an organized summary of the published literature concerning gas-phase negative ion–molecule reactions of transition-metal species. The main focus will be on investigations of gas-phase reactions, their mechanisms, and the thermochemical information for transition-metal ions and molecules that may be derived from such studies. The general re-

0009-2665/87/0787-0623$06.50/0

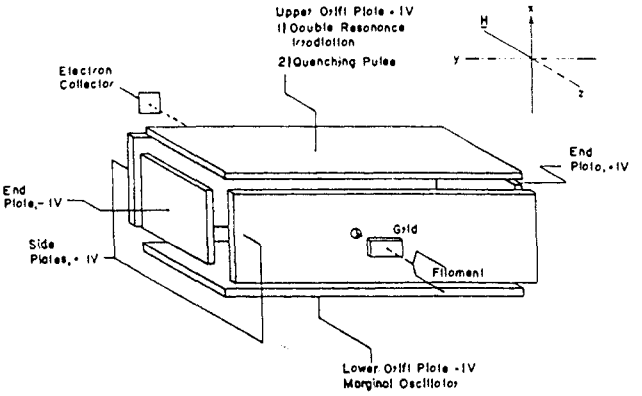

Figure 1. Schematic diagram of an ICR cell. Reprinted with permission from McIver, R. T., Jr. *Rev. Sci. Instrum.* 1970, *41*, 555. Copyright 1970 American Institute of Physics.

activity trends which emerge from the assembled work on negative metal ion chemistry will be highlighted, with the hope that they might inspire additional studies. Coverage includes published and some unpublished material through 1986.

II. Experimental Techniques

Most of the experimental work on negative metal ion chemistry has been carried out with the use of ion cyclotron resonance spectrometry (ICR), flowing afterglow techniques (FA), and Knudsen cell mass spectrometry. A brief summary of the basic operating principles of ICR, FA, and allied experimental methods is provided here, along with some discussion concerning the relative merits and shortcomings of each for the study of negative metal ion chemistry.

A. Ion Cyclotron Resonance

The ion cyclotron resonance technique and its recent offspring Fourier transform ICR (FT-ICR, sometimes referred to as FTMS) account for the largest number of gas-phase metal ion studies. A simplified schematic diagram of a conventional ICR cell is illustrated in Figure 1.[8] The reaction vessel consists of a cubic or rectangular cell, typically 2–5 cm on a side, which is housed in a vacuum can fitted between the pole faces of an electro- or superconducting magnet. Ions are usually produced within the cell by electron impact ionization of the sample gas which is present as a static background pressure at 10^{-7} to 10^{-6} Torr. At the 0.9–3.0 T magnetic fields normally employed, the ions are constrained to cyclic orbits with cyclotron frequencies in the radio frequency (rf) range as given by eq 1, where

$$\omega_c = B(q/m) \quad (1)$$

ω_c is the cyclotron frequency, B is the magnetic field strength, and q/m is the charge-to-mass ratio of the ion. Trapping potentials on the side plates of the cell are used to confine ions of the desired polarity, and relatively high concentrations of reactive ions can be maintained for long periods of time (several seconds). During a variable-length trapping interval prior to detection, ion–molecule reactions may take place with the background sample or with other reagent gases added to the system via metering-valve inlets. In the conventional (continuous wave) ICR experiment, detection of ions is achieved by sweeping the magnetic field and

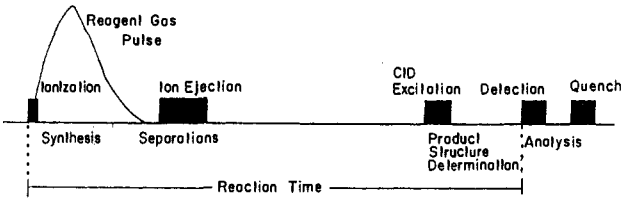

Figure 2. Typical FTMS pulse sequence for generating an ion by electron impact, isolating the ion in the cell by double-resonance ejection pulses, collisionally activating the ion by application of a resonant pulse of medium power, and final detection of the resulting fragment ions. Reprinted with permission from Jacobson, D. B.; Freiser, B. S. *J. Am. Chem. Soc.* 1984, *106*, 3900. Copyright 1984 American Chemical Society.

successively bringing ions of different mass into resonance with an external rf (marginal) oscillator. Newer detection modes employ frequency-scanning[9] and/or capacitance bridge detectors.[10]

One of the most important advances in ICR spectroscopy is the development of the Fourier transform technique by Comisarov and Marshall in 1974.[11] This powerful operation mode permits the collection of a complete mass spectrum of ions in the cell with application of a single low-energy rf pulse. A typical operational cycle for an FT-ICR (FTMS) experiment is shown in Figure 2. It is comprised of a sequence of rf pulses of varying amplitude with intervening delay periods followed by a final detect pulse. Reagent gases may be present as a static pressure or pulsed into the cell during particular reaction delay periods.[12] Ions of a desired mass or range of masses may be ejected from the cell by the application of high-energy rf pulses at the appropriate discrete frequencies, thus permitting the study of ion–molecule reactions with a single pure reagent ion and the identification of precursor ions for a particular product ion ("double resonance"). Collision-induced dissociation (CID) experiments in the FT-ICR are performed by translational excitation of the desired parent ion with a medium-power rf pulse in the presence of a relatively high background pressure of an inert target gas such as argon ($P \simeq 2 \times 10^{-6}$ Torr).[13] Multiple activating collisions of the excited ion result in its fragmentation, and the daughter ions produced in this way remain trapped in the cell for subsequent detection or reaction. CID provides both a valuable tool for analysis of ion structure and a useful means for preparing novel ions for further study.[14]

The key strengths of the ICR and FT-ICR methods in the study of negative metal ion chemistry are (1) complex reaction sequences can be sorted out with double-resonance ejection procedures for isolating a reactive ion or establishing a reactant ion/product ion connection; (2) pulsed-valve reagent inlets can permit the study of metal ion reactions in the absence of potentially reactive neutral precursors; (3) a variety of ion source configurations may be employed, including solid probes and laser desorption;[15] (4) the low pressure in the system permits direct use of relatively involatile metal compounds; and (5) quite high resolution and high mass ranges may be achieved.[16]

ICR-based methods are not without certain disadvantages. Because of the low pressure in the reaction cell, there is uncertainty regarding the energy distribution of the trapped ions. The possibility exists that residual kinetic, vibrational, and electronic excitation remains in the ions following their formation that is not

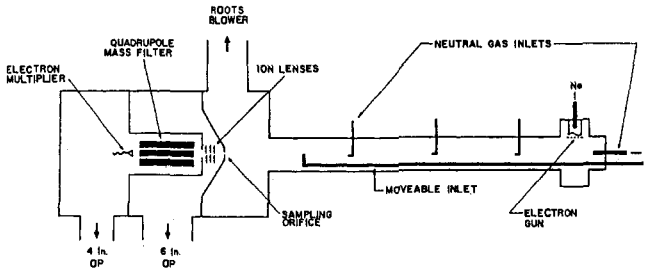

Figure 3. Simplified schematic diagram of a flowing afterglow apparatus.

quenched by the limited trapping periods usually allowed for collisional cooling[8] (e.g., 100 ms at 10^{-6} Torr corresponds to less than five ion–molecule collisions per ion). Furthermore, for negative ion studies the presence of trapped electrons in the cell can be problematic since reionization of the metal ion neutral precursor(s) may take place during the ion–molecule reaction period. Identification of reactions and measurement of rates can become quite difficult under these conditions. Electron ejection procedures have been adopted in some laboratories;[17] however, this practice does not appear to be widespread.

B. Flowing Afterglow

The flowing afterglow method[18,19] is a relative newcomer to gas-phase transition-metal ion chemistry, with the first negative ion applications appearing only a few years ago. The basic flowing afterglow configuration is illustrated in Figure 3. Ions are produced at the upstream end of a linear flow reactor by electron impact ionization of neutral precursors. A fast-flowing buffer gas (usually helium) also enters the instrument in this region and carries the ions through the flow tube. At the buffer gas pressures usually employed (0.1–1.0 Torr), the ions become thermally equilibrated with the room temperature bath and achieve a thermal energy distribution within 10–15 cm of the ion source. The flowing plasma is sampled through an orifice in a nosecone at the downstream detection end, and ions of the desired charge are focused into a quadrupole mass spectrometer. Thus, a mass spectrum representing the steady-state ion composition in the flow tube can be obtained. Ion–molecule reactions are initiated in the reactor by the addition of small flows of neutral reagent gases through fixed inlets located at regular intervals along the length of the tube. Moveable neutral inlets are used in some instruments for continuous variation of the reaction distance. Bimolecular reaction rate coefficients are readily measured under pseudo-first-order conditions by monitoring the decay of a reactive ion as a function of either the reaction distance or the neutral flow rate.[19]

The main advantages of the flowing afterglow method for negative metal ion studies stem from the relatively high pressure in the reactor. Not only is thermalization of the reactant ions generally assured, but the higher pressure also facilitates termolecular addition reactions between ions and molecules,[20] thereby allowing the formation of metal ion species that may not be readily accessible in lower pressure experiments. Reliable kinetic measurements can be made in a flowing afterglow with estimated accuracies for rate constants of ±20% and precision typically better than ±5%.[21] Also, because of the flow nature of the technique, reactive or metastable species formed in microwave discharges or flow-pyrolysis inlets may be used as the neutral components in gas-phase ion–molecule reactions.[22] Some disadvantages of FA are the limited resolution and mass range of the usual quadrupole mass analyzers, the requirement for fairly volatile neutral compounds that are available in large quantities, and the potential problems associated with the presence of free electrons in the reaction region of the flow tube.

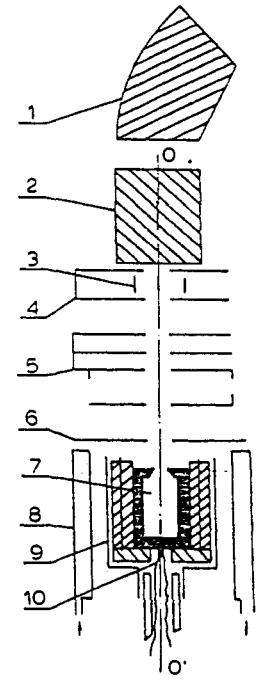

Figure 4. Effusion cell mass spectrometer for examining ion–molecule equilibria at high temperatures: (1) magnet; (2) deflection plates; (3) correction plates (±150 V); (4) collimating slits; (5) focusing lens; (6) drawing-out lens (−1700 to −2000 V); (7) effusion cell (−2000 V); (8) water jacket; (9) heater; (10) thermocouple. Reprinted with permission from ref 24. Copyright 1980 Elsevier Science Publishers.

C. Knudsen Cell Methods

High-temperature mass spectrometry is an important and time-honored technique for investigating equilibrium reactions involving inorganic compounds.[23] More recent applications have utilized effusion mass spectrometry in conjunction with Knudsen cells to characterize the negative ion–molecule equilibria taking place in the saturated vapor over binary mixtures containing transition-metal compounds. The technique is especially well suited for assaying equilibria involving relatively stable species that possess high electron affinities and/or large heterolytic and homolytic bond strengths. Sidorov and co-workers have extensively developed this technique for measurements of heats of formation of binary fluoride ions (MF_n^-), fluoride ion affinities (D-$[MF_n$–$F^-]$) and high electron affinities (EA > 5.0 eV).[24,25] A simplified schematic diagram of the system employed in most of these studies is shown in Figure 4. It consists of a nickel effusion cell that may be heated to more than 1100 K, an effusion orifice, provisions for ion optics, and a single-focusing mass spectrometer. The sample, which may consist of any of a variety of binary fluoride systems such as NaF–FeF_3 or AlF_3–NiF_2 or pure salts such as K_2CrO_4, is loaded into the cell, and

heating to ca. 900–1000 K produces a saturated vapor composed of ions and neutral molecules in concentrations that are dictated by the equilibrium constants for sublimation, dissociation, and ion–molecule reaction. For negative ion studies, the effective work function of the inner surface of the effusion chamber must be decreased to enhance the concentration of negative ions in the saturated vapor.[24] This is accomplished by adding alkali-metal vapors to the cell or incorporating in the sample alkali-metal compounds that yield free metal upon dissociation or reduction. The negative ions in the cell are extracted with a draw-out field, and their relative abundance is determined with the mass spectrometer. Concentrations of neutral components in the cell are usually deduced from literature specifications of saturated-vapor composition as a function of temperature. More recently, Sidirov and co-workers have employed direct EI ionization in the effusion chamber to determine neutral concentrations from the observed positive ion currents that result.[26] Evaluation of the separate equilibrium constants that control the observed neutral concentrations and ion abundance ratios is used in conjunction with van't Hoff analysis of their temperature dependence to derive the reaction enthalpies of interest.

Knudsen cell methods are limited to fairly robust compounds that are capable of withstanding high temperatures (>500 K) without extensive decomposition. The thermochemical data derived from equilibrium studies of such species may be very high quality (e.g., ±1.0 kcal in a given reaction enthalpy), and the technique may be used to obtain thermochemistry for ion–molecule reactions, neutral–neutral reactions, and even ion–ion reactions.[24,27]

III. Atomic Negative Ions

Atomic negative ions have been formed from most all transition-series elements that possess bound anion states. Accurate electron affinities for neutral metal atoms and detailed information about the electronic structures of the corresponding atomic anions have been obtained from laser photoelectron measurements and allied techniques.[28] The most commonly employed source of atomic metal anions for these studies is the cesium sputter-ion source of the type originally developed for tandem accelerators.[29] While high concentrations of atomic metal negative ions are available from these sources, they have not been used in conjunction with instrumentation equipped for ion–molecule-reaction studies. Moreover, the usual electron impact, surface ionization, or laser desorption methods used for producing atomic metal cations do not generally yield sufficient quantities of atomic anions to permit the examination of their reactions. Accordingly, there are only a few accounts of atomic transition-metal-anion reactions presently available.

In 1983, Squires and Freiser reported a new method for preparing atomic transition-metal anions under conditions where their subsequent reactions with neutral substrates could be examined.[30] Collision-induced dissociation of simple metal carbonyl negative ions in an FTMS was found to produce atomic anion fragments in good yield (eq 2). The metal carbonyl anions used as precursors are easily prepared from electron impact on the corresponding neutral carbonyl complexes. The CID method was applied to the generation of V^-, Cr^-, Fe^-, Co^-, Mo^-, and W^- from $V(CO)_5^-$, $Cr(CO)_5^-$, $Fe(CO)_4^-$, $Co(CO)_4^-$, $Mo(CO)_5^-$, and $W(CO)_5^-$, respectively.[31] Collisional activation of $Mn(CO)_5^-$ (from $Mn_2(CO)_{10}$) did not produce an observable Mn^- signal, in accordance with the predicted instability of this ion toward electron autodetachment.[28] Figure 5 shows a sequence of Fourier transformed mass spectra illustrating the formation and subsequent isolation of Cr^- by the CID method. Addition of neutral samples to the FTMS cell enabled examination of the ion–molecule reactions of the atomic anions. Since the parent metal carbonyl complexes were always present in the system as a background pressure, their reactions with the atomic ions were extensively characterized. Dissociative electron transfer is the major reaction observed in each system (eq 3–7), and clustering reactions to form di-

$$M(CO)_n^- \xrightarrow{CID} M^- + nCO \quad (2)$$

$$V^- \xrightarrow{V(CO)_6} V(CO)_5^-,\ V_2(CO)_3^-,\ V_2(CO)_4^-,\ V(CO)_6^- \quad (3)$$

$$Cr^- \xrightarrow{Cr(CO)_6} Cr(CO)_5^-,\ Cr_2(CO)_5^- \quad (4)$$

$$Fe^- \xrightarrow{Fe(CO)_5} Fe(CO)_4^- \quad (5)$$

$$Co^- \xrightarrow{Co_2(CO)_8} Co(CO)_4^-,\ Co_2(CO)_6^-,\ Co(CO)_3^-,\ Co_2(CO)_5^- \quad (6)$$

$$Mo^- \xrightarrow{Mo(CO)_6} Mo(CO)_5^-,\ Mo_2(CO)_4^- \quad (7)$$

nuclear carbonyl anions are evident for all but Fe^-. Certain of the cluster ions exhibit behavior suggestive of unusual structures (cf. section V). For example, the $Cr_2(CO)_5^-$ ion produced in eq 4 was found to fragment when collisionally activated by exclusive loss of Cr (eq 8), while the divanadium ions formed by eq 3 fragment by complete decarbonylation (eq 9). This was inter-

$$Cr_2(CO)_5^- \xrightarrow{CID} Cr(CO)_5^- + Cr \quad (8)$$

$$V_2(CO)_{3,4}^- \xrightarrow{CID} V_2^- + 3,4CO \quad (9)$$

preted in terms of a relatively loosely bonded chromium atom ligand in an unsymmetrical structure for $Cr_2(CO)_5^-$ and stronger multiple metal–metal bonds in the divanadium clusters.

The atomic metal anions were found to be completely unreactive in the presence of saturated and unsaturated hydrocarbons, failing to show any of the oxidative insertion-reductive elimination chemistry that is so prevalent with atomic metal cations.[32] The likely origin of this difference in reactivity is the fact that most all of the atomic metal anions possess $d^n s^2$ electronic configurations in which the (diffuse) valence s orbital is doubly occupied,[28] while the metal cations are relatively contracted species with d^n or $d^{n-1}s^1$ configurations.[33] As a result, electron–electron repulsion between the negative metal ion and a neutral substrate may accrue at greater distances than with positive ions, thereby impeding efficient interaction between the appropriate metal and substrate orbitals required for C–H or C–C insertion. In addition, since it has frequently been noted that a half-filled valence s orbital (or p orbital) in metal cations is a prerequisite for facile insertion reactions[34] and/or strong metal–ligand bonds,[35] then

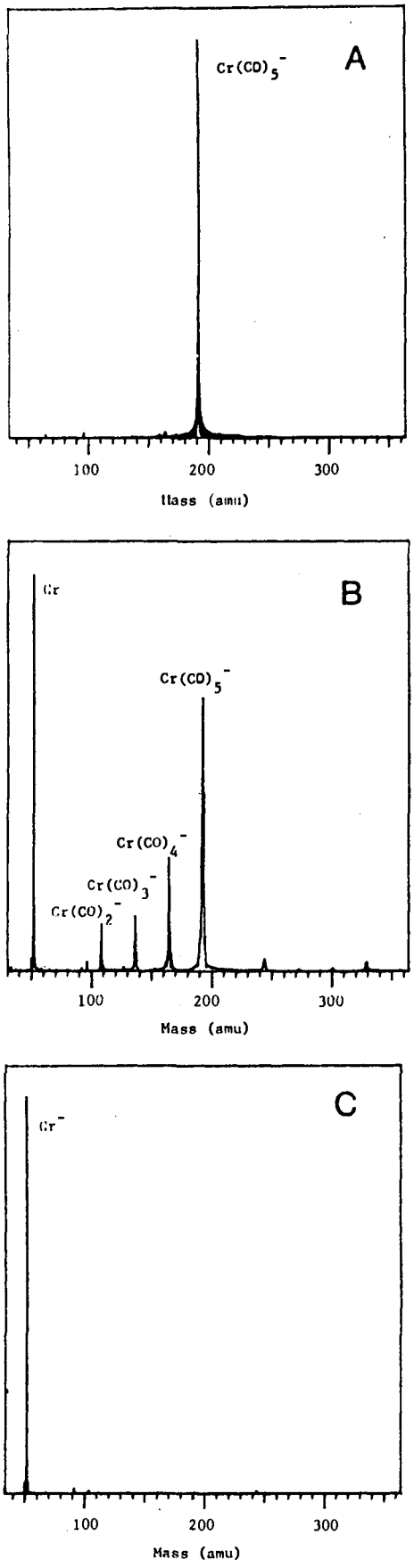

Figure 5. Fourier-transformed mass spectra illustrating the generation of Cr^- from (A) electron impact ionization of $Cr(CO)_6$, (B) collision-induced dissociation of $Cr(CO)_5^-$ by translational excitation in the presence of Ar collision gas and (C) double-resonance ejection of all ions from the FTMS cell except Cr^-. Reprinted with permission from ref 30. Copyright 1983 American Chemical Society.

TABLE I. Metal Anion Proton Affinities and M-H Homolytic Bond Dissociation Energies[a]

M	PA(M^-), kcal	D[M–H], kcal
Fe	339.4 ± 3	29.6 ± 3
V	339.4 ± 3	37.9 ± 3
Cr	339.4 ± 3	41.2 ± 3
Co	340.5 ± 3	42.2 ± 3
Mo	342.4 ± 3	46.0 ± 3

[a] Taken from ref 31.

atomic anions would be expected to be less reactive since their $d^{n+1}s^1$ states (and p states) generally lie significantly higher in energy than the d^ns^2 ground states.[28] That is, the promotion-energy term in the energy barrier for oxidative insertion is probably large.

While the atomic anions fail to react with simple hydrocarbons, they do undergo proton-transfer reactions with relatively strong acids (eq 10). Proton af-

$$M^- + HX \rightarrow MH + X^- \quad (10)$$

finities (PA) for V^-, Cr^-, Fe^-, Co^-, and Mo^- were bracketed from the observation of proton-transfer reactions with a series of reference acids possessing established gas-phase acidities.[31] The metal anions were found to be relatively weak bases, with proton affinities comparable to those of carboxylate and thiolate ions. Table I summarizes the measured basicities for five metal anions along with the corresponding homolytic bond strengths for the diatomic metal hydrides, D[M–H], derived from eq 11. Additional thermochemical

$$PA(M^-) = \Delta H_{acid}(MH) = D[M\text{–}H] - EA(M) + IP(H) \quad (11)$$

properties were derived from the new PA(M^-) values, including $\Delta H_f°$[MH,g], IP(MH), D[M^-–H], and D[M–H^-]. A notable feature of the measured metal anion basicities listed in Table I is that they are all virtually the same (340 ± 2 kcal/mol).

The generality of the trend noted above was established in a companion paper by Squires.[36] Compiling measured and calculated M–H bond strengths from the literature and combining them with metal atom electron affinities according to eq 11 gave an expanded list of diatomic metal hydride acidities. The values generally fall within a narrow range of 341 ± 5 kcal/mol, just as with the directly measured acidities listed in Table I. This interesting uniformity in the acidities is evidently unique to the transition-series elements since main-group diatomic hydrides and alkali hydrides possess widely varying gas-phase acidities.[37] Moreover, metal hydride cations (MH^+)[35] and metal hydride complexes (L_nMH)[38] also exhibit a wide range of thermodynamic acidities. In terms of eq 11, constant MH acidity must arise from a correlation between electron affinity and MH homolytic bond energy for the transition-series elements. A plot of EA(M) vs. D[M–H] constructed with the currently available data substantiates this conclusion.[39] It was shown that the observed linear relationship (D[M–H] = EA(M) + 27.5 kcal/mol) could be used to estimate metal–hydrogen bond strengths from measured metal atom electron affinities. The origin of the trend was discussed by Squires in terms of a formal analogy that can be drawn between the electron configuration of atomic metal anions and their corresponding diatomic hydride. That is, formation of most atomic negative ions and neutral metal hydrides

from transition-metal atoms generally results in an electron configuration characterized by an additional (nonbonding) d electron and a stabilized, doubly-occupied s or σ orbital. Further refinements of the correlation model in terms of the relevant electronic promotional energies and ionization potentials were also provided.

In related studies, Weil and Wilkins prepared Au^- in an FTMS by laser desorption from gold-plated targets and determined its proton affinity by the bracketing technique.[40] The gas-phase acidity of AuH was determined to be 331 ± 3 kcal/mol, a value which is in good agreement with that calculated with use of eq 11 and the well-established electron and hydrogen-atom binding energies for gold.

IV. Negative Metal Ion Fragments and Complexes

The majority of gas-phase negative metal ion studies have focused on the reactions of transition-metal-containing anions that possess coordinated ligands. For the purposes of this review, metal anion complexes and "fragments" will be defined to include all such negative metal ions that contain one or more organic or inorganic ligand, irrespective of the degree of coordinative saturation or unsaturation of the metal. The particular reactions of metal anions with neutral metal compounds that yield polynuclear products will be deferred to a later section on cluster ions (section V).

A. Ion Formation and Thermochemistry

Transition-metal negative ion fragments and complexes are derived from a variety of sources. Electron impact ionization (EI) of volatile metal compounds is the most commonly used method and, depending upon the source pressures, electron energies, and substrates used, will produce molecular anions and/or smaller fragment ions from direct or dissociative electron capture and ion-pair formation.[4] A comprehensive review of electron impact processes involving transition-metal and main-group organometallic compounds has been prepared by Gregor and Guilhaus, and the reader is referred to this work for more detailed information concerning negative ion formation mechanisms.[41]

Ionization processes involving simple metal carbonyl complexes are of particular relevance here since the EI-derived fragment ions from these compounds have received the greatest amount of attention with respect to metal ion–molecule reactions. Saturated (18-electron) mononuclear metal carbonyls generally yield 17-electron negative ion complexes via dissociative electron capture with thermal energy electrons (eq 12).[42] Parent

$$M(CO)_n \xrightarrow{e^-(\text{thermal})} M(CO)_{n-1}^- + CO \qquad (12)$$

molecular anions are usually not observed, although their transient existence has been inferred from electron transmission spectroscopy studies.[43] Increasing the electron energy results in more extensive fragmentation, with the progression of maxima in the yield curves for the successively decarbonylated fragment ions suggesting resonance-capture mechanisms.[42,44] Thus, in low-pressure (ICR) studies of reactions involving specific metal carbonyl anions, it is necessary to use low electron energies (1–5 eV) near the resonance-capture maxima in order to optimize formation of the desired fragment anion.[41] In contrast, with higher pressure sources (such as in a flowing afterglow) that involve significantly lower and broader electron energy distributions, it has been found necessary to use very high emission currents (ca. 10 mA) in order to achieve sufficient quantities of electrons with the appropriate energies to produce the more highly dissociated metal carbonyl fragment ions.[45]

Dinuclear and higher nuclearity metal carbonyl complexes undergo low-energy electron impact fragmentation by both metal–metal and metal–carbonyl bond cleavage. For example, $Mn_2(CO)_{10}$ produces mainly the 18-electron $Mn(CO)_5^-$ ion and significant quantities of $Mn_2(CO)_{8,9}^-$ fragments from 5-eV EI at low pressure, while the congeneric complex $Re_2(CO)_{10}$ yields exclusively $Re_2(CO)_9^-$ under the same conditions.[46] Transition-metal carbonyl complexes bearing other ligands such as hydrogen, halogen, or alkyl also ionize by dissociative electron capture in which mainly neutral CO ligands are expelled.[41] When larger, multidentate organic ligands such as polyenes or arenes are coordinated with the metal, low-energy electron capture may produce parent molecular anions. This is made possible by the ability of such complexes to accommodate the extra electron through a partial reduction in the bond order between the metal and the organic ligand ("slippage").[47] For example, while $Fe(CO)_5$ yields mainly $Fe(CO)_4^-$ (and traces of $Fe(CO)_3^-$) from thermal energy electron capture, the η^4-1,3-butadiene complex produces an abundant molecular anion (eq 13).[48] The

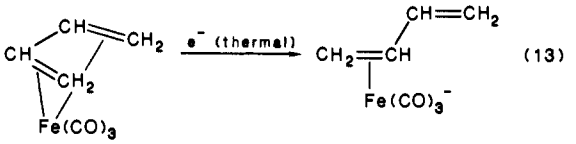

(13)

corresponding metal ion complex has been produced in solution,[49,50] and a structure incorporating an η^2-butadiene ligand has been proposed.

In the context of gas-phase ion–molecule reactions, the most significant physical properties of metal anion fragments and complexes that need to be considered are the electron affinities, proton affinities, and metal–ligand bond strengths. These data provide the thermochemical constraints on most conclusions made regarding reactivity, mechanism, and product ion structures. Only limited data of this type are presently available, although with each new study involving negative metal ion chemistry the database has grown. As described in the previous section, atomic transition-metal anions are relatively weak bases ($PA(M^-) \simeq$ 340 kcal/mol) with electron binding energies ranging from ≤0 eV (Mn) to 2.3 eV (Au).[28] Addition of CO ligands to the metal may increase or decrease the electron affinity of the complex relative to the bare metal. For example, as shown in Table II the measured electron affinities for the series of iron carbonyls $Fe(CO)_n$ generally increase with increasing n,[51] while for the nickel series the electron affinity initially decreases for Ni(CO) and $Ni(CO)_2$ and then increases for $Ni(CO)_3$.[52] A regular increase in electron affinity with increasing numbers of CO ligands has also been measured for chromium and tungsten carbonyls.[53]

While only few in number, measurements of gas-phase acidities for metal carbonyl hydride complexes

TABLE II. Electron Binding Energies and Proton Affinities of Transition-Metal Negative Ions

species, ML_n	EA(ML_n), eV	ref	PA(ML_n^-), kcal	ref
Fe	0.16 ± 0.04	28	339.4 ± 3	31
Fe(CO)	1.26 ± 0.02	51		
$Fe(CO)_2$	1.22 ± 0.02	51		
$Fe(CO)_3$	1.8 ± 0.2	51		
$Fe(CO)_4$	2.4 ± 0.3	51	≥319 ± 5	2
$HFe(CO)_4$			319 ± 5	2
Ni	1.16 ± 0.01	28	346.9 ± 3	36
Ni(CO)	0.804 ± 0.012	52		
$Ni(CO)_2$	0.643 ± 0.014	52		
$Ni(CO)_3$	1.077 ± 0.013	52		
Co	0.661 ± 0.010	28	340.5 ± 3	31
$Co(CO)_4$	≥2.3	2	≤314	2
Mn	≤0	28	≥355	36
$Mn(CO)_5$	2.43 ± 0.21	46	318 ± 3	2

suggest that CO coordination to a metal anion considerably reduces its thermodynamic basicity (Table II). For instance, the proton affinities measured for $Fe(CO)_4^-$ (PA > 319 ± 5 kcal/mol),[2] $HFe(CO)_4^-$ (PA = 319 ± 5 kcal/mol),[2] $Co(CO)_4^-$ (PA < 314 kcal/mol), and $Mn(CO)_5^-$ (PA = 318 ± 3 kcal/mol)[2] are more than 20 kcal/mol less than those of the corresponding atomic anions (section III). In terms of eq 11, the decreased proton affinities of the metal carbonyl anion complexes can be attributed to their larger electron binding energies compared to the bare metal anions. This, in turn, is most likely due to the extensive charge delocalization (and, hence, stabilization) in the carbonyl anions due to M(d)–CO(π^*) backbonding.[54,55] Because of their low basicities, high electron binding energies, and delocalized negative charge, metal carbonyl anions are expected to be exceptionally poor nucleophiles in gas-phase displacement and addition reactions.

Metal–ligand bond strengths for negative ion complexes and fragments are also relatively scarce (Table III). Appearance energy measurements are available for iron carbonyl ions ($Fe(CO)_n^-$, n = 0–4),[44] nickel carbonyl ions ($Ni(CO)_n^-$, n = 0–3),[44] and certain of the group 6 metal carbonyl ions ($M(CO)_n^-$, M = Cr, Mo, W; n = 0–5).[56] The differences within each series provide estimates of the successive metal–carbonyl bond strengths for the ions, $D[M(CO)_{n-1}^-–CO]$. The bond energy orderings in the iron and nickel series have been discussed in detail by Lineberger.[51,52,57] Appearance energies for a few other metal ion fragments are available from which metal–hydrogen, metal–oxygen, and metal–halogen bond strengths may be derived.[4] Additional data may be obtained by combining known bond energies for neutral complexes and fragments with

TABLE III. Metal–Ligand Bond Strengths in Negative Ion Complexes and Fragments

ML_n	$D[M^-–L]$,[a] kcal	ref	$D[M–L]$,[a] kcal	ref
Metal–Carbonyl, L = CO				
$Fe(CO)_5$			41.5 ± 2.0	76
$Fe(CO)_4$	18 ± 7	51	4.6 ± 9.2	51
$Fe(CO)_3$	46 ± 5	51	32 ± 7	51
$Fe(CO)_2$	23 ± 7	51	23 ± 7	51
Fe(CO)	46 ± 7	51	21 ± 7	51
$Ni(CO)_4$			25 ± 2	52
$Ni(CO)_3$	23 ± 9	52	13 ± 10	52
$Ni(CO)_2$	51 ± 15	52	54 ± 15	52
Ni(CO)	21 ± 15	52	29 ± 15	52
$Cr(CO)_6$			36.8 ± 2.0	76
$Cr(CO)_5$	12	56	<7	56, 53
$Cr(CO)_4$	55	56	42	56, 53
$Cr(CO)_3$	35	56	27	56, 53
$Cr(CO)_2$	35	56		
Cr(CO)	20	56		
$Mo(CO)_6$			40.5 ± 2.0	76
$Mo(CO)_5$	16	56		
$Mo(CO)_4$	37	56		
$W(CO)_6$			46.0 ± 2.0	76
$W(CO)_5$	20	56	<20	56, 53
$W(CO)_4$	32	56	29	56, 53
$W(CO)_3$	5	56	4	56, 53
Metal–Hydrogen, L = H				
CrH			41.2 ± 3	31
FeH	47.4 ± 3	57	29.6 ± 3	31
CoH	42.5 ± 3	57	42.2 ± 3	31
NiH	44.4 ± 3	57	60 ± 3	36
$(CO)_4FeH$	70 ± 14	2		
Metal–Oxygen, L = O				
CrO	105	64	101	64
OCr–O	149	64	125	64
FCr–O	131	64	138	64
ClCr–O	127	64	125	64
FOCr–O	143	64	99	64
ClOCrO	129	64	101	64
$F_2Cr–O$	125	64	113	64
$Cl_2Cr–O$	115	64	99	64
$F_2OCr–O$	58	64	106	64
$Cl_2OCr–O$	58	64	111	64
FeO	129	58	98	59

ML_n	$D[M^-–L]$,[a] kcal	ref	$D[M–L]$,[a] kcal	ref
Metal–Halogen, L = F, Cl, Br, I				
CrF	104	64	106	64
CrCl	85	64	88	64
OCr–F	131	64	143	64
OCr–Cl	104	64	111	64
$O_2Cr–F$	125	64	118	64
$O_2Cr–Cl$	88	64	88	64
$FCr–F$	131	64	120	64
$ClCr–Cl$	115	64	99	64
FOCr–F	127	64	95	64
ClOCr–Cl	104	64	74	64
$FO_2Cr–F$	42	64	101	64
$ClO_2Cr–Cl$	30	64	83	64
$(CO)_5Cr–Cl$	>79.2	84		
$(CO)_5Cr–Br$	>70.6	84		
$(CO)_5Cr–I$	>57.2	84		
$(CO)_4MnCl–Cl$	>70.3	84		
$(CO)_4MnCl–Br$	>70.6	84		
$(CO)_4MnBr–Cl$	>70.3	84		
$(CO)_4MnBr–Br$	>70.6	84		
$(CO)_4MnBr–I$	>55.0	84		
$(CO)_4ReCl–Cl$	>79.2	84		
$(CO)_4ReCl–Br$	>70.6	84		
$(CO)_4ReCl–I$	>57.2	84		
$(CO)_4ReBr–Cl$	>79.2	84		
$(CO)_4ReBr–Br$	>70.6	84		
$(CO)_4Br–I$	>57.2	84		
$(\eta^3\text{-}C_3H_5)Mn(CO)_3–Cl$	>70.3	84		
$(\eta^3\text{-}C_3H_5)Mn(CO)_3–I$	>57.2	84		
$(\eta^3\text{-}C_3H_5)Re(CO)_3–Cl$	>82.8	84		
$(\eta^3\text{-}C_3H_5)Re(CO)_3–Br$	>70.6	84		
$(\eta^3\text{-}C_3H_5)Re(CO)_3–I$	>57.2	84		
$(CO)_4Fe–Cl$	79 ± 6	60		
$(CO)_4Fe–Br$	>69	60		
$(CO)_4Fe–I$	>54	60		

[a] Uncertainties given only when available in the original report.

the appropriate electron affinities. For example, the recently measured[58] EA(FeO) = 34.4 ± 0.5 kcal/mol may be combined with D[Fe–O] = 98 ± 4 kcal/mol[59] and EA(Fe) = 3.7 ± 0.8 kcal/mol[28] according to eq 14

$$D[Fe^-–O] = D[Fe–O] + EA(FeO) - EA(Fe) \quad (14)$$

to yield $D[Fe^-–O]$ = 129 ± 4 kcal/mol. The observation of certain ion–molecule reactions may also be used to infer limits on metal–ligand bond strengths. McDonald and co-workers have derived limits for iron–halogen bond strengths in the tetracarbonyliron complexes $XFe(CO)_4^-$ (X = Cl, Br, I) and various group 7 metal ion complexes from the occurrence of halogen atom abstraction from halomethanes.[60,84] The metal–hydrogen bond energy in the tetracarbonyliron hydride complex $D[(CO)_4Fe^-–H]$ = 70 ± 14 kcal/mol may be derived from the measured acidity of $H_2Fe(CO)_4$ (ΔH_{acid} = 319 ± 5 kcal/mol),[2] an estimate for $\Delta H_f°[H_2Fe(CO)_4,g]$ = −132 ± 6 kcal/mol,[61] and $\Delta H_f°[Fe(CO)_4^-,g]$ = −161 ± 10 kcal/mol.[51] It is interesting to note that this bond energy is nearly 25 kcal/mol greater than that for the diatomic hydride FeH^- ($D[Fe^-–H]$ = 47.3 ± 3 kcal/mol).[62] A significant difference in the type of Fe–H bonding orbitals used in the two ions is suggested by this result.

A large number of electron and fluoride ion affinities for binary transition-metal fluorides as well as metal polyfluoride ion heats of formation have been determined equilibrium Sidorov and his associates from fluoride ion and electron-transfer equilibria measurements in a Knudsen cell mass spectrometer. A recent compilation of these data may be found in ref 25.

An extensive list of new thermochemical data for iron tetracarbonly acyl anion complexes $(CO)_4FeC(O)X^-$ was recently reported by Lane, Sallans, and Squires.[63] Measurements of the $Fe(CO)_5$ binding energies of a series of negative ions, $D[(CO)_4FeCO–X^-]$, revealed a linear correlation between the proton affinity of X^- and its energy of attachment to $Fe(CO)_5$ (eq 15). The

$$D[(CO)_4FeCO–X^-] = 0.66\ PA(X^-) - 206\ kcal/mol \quad (15)$$

correlation was shown to operate over a wide range of bond energies—from the strongly basic hydride ion $D[(CO)_4FeCO–H^-]$ = 56.1 ± 4 kcal/mol, $PA(H^-)$ = 400.4 kcal/mol,[37] to the weakly basic choride ion $D[(CO)_4FeCO–Cl^-]$ = 13.9 ± 3 kcal/mol, $PA(Cl^-)$ = 333.4 kcal/mol.[37] Binding energies of negative ions to $Fe(CO)_5$ may be used to derive estimates for the heats of formation of the corresponding iron–acyl anions, provided in thermochemistry for the anion X^- is known.

B. Reactions

The earliest reports of ion–molecule reactions involving transition-metal negative ions mainly dealt with the specific processes taking place with EI-derived fragment ions and their parent neutral metal compound. Explicit treatment of the self-condensation (clustering) reactions of this type that produce polynuclear cluster ions will be given in section V. Atom abstraction reactions involving gaseous metal anions were known as early as 1969.[64] Flesch, White, and Svec identified the oxygen and halogen atom transfer reactions shown in eq 16 and 17 from the negative ion mass

$$CrO_2X^- + CrO_2X_2 \rightarrow CrO_3X^- + CrOX_2 \quad X = F, Cl \quad (16)$$

$$CrOX_2^- + CrO_2X_2 \rightarrow CrOX_3^- + CrO_2X \quad X = F, Cl \quad (17)$$

spectra of CrO_2F_2 and CrO_2Cl_2 obtained with the source operating at relatively high pressure (ca. 2×10^{-6} Torr). Careful analysis of the product ion yields as a function of the ionization energy and source pressure established the precursor ions for the observed products as indicated. The appearance of trace amounts of $CrO_2X_2^-$ ions in the spectra was also noted and was attributed to atom abstraction or charge exchange with the parent gas in the source.

The subsequent deliberate attempts to investigate reactions of negative metal ions with neutral substrates appearing over the past 20 years are conveniently organized into three main categories: ligand substitution and addition reactions, oxidation reactions with dioxygen, and oxidative insertion/reductive elimination reactions.

1. Ligand Substitution and Addition

Extensive accounts of gas-phase ligand-exchange reactions involving positive metal ion fragments and complexes have been published which provide useful information about relative metal–ligand bond strengths.[2,65] A few reports involving negative metal ion complexes are also available. Before describing these studies, it is worthwhile to consider here a few distinctive mechanistic features of gas-phase ligand substitution and addition reactions with metal ions: (A) Ligand-exchange reactions occurring in solution are generally assigned either a dissociative or an associative mechanism, depending ultimately upon the molecularity and the change in metal coordination number in the rate-determining step (eq 18).[66] In the gas phase,

$$L'ML_{n-1} \xleftarrow{-L} \underset{\text{associative}}{(L'ML_n)} \xleftarrow{+L'} ML_n \xrightarrow{-L} \underset{\text{dissociative}}{(ML_{n-1})} \xrightarrow{+L'} L'ML_{n-1} \quad (18)$$

ligand-exchange reactions necessarily proceed through associative mechanisms since they are strictly bimolecular processes involving thermalized reactants with constant total energy. That is, prior "unimolecular" dissociation of a ligand from an isolated metal ion complex cannot occur once it is formed and thermally equilibrated since insufficient energy is available in the reacting system. Of the several alternatives for the obligatory associative mechanism, associative interchange (I_a) occurring with ligand slippage, electron transfer or through hyperelectronic (≥19 electron) metal ion intermediates is conceivable.[66] (B) The occurrence of displacement of ligand L by L′ in a reactive metal ion complex ML_{n+1}^- requires that $D[L'–ML_n^-] > D[L–ML_n^-]$ since only exothermic reactions ($\Delta H < 0$) may occur in the gas phase when the overall entropy change is small.[67] This principle may be exploited in the construction of scales of relative metal–ligand binding energies from qualitative observations of the favored direction for ligand substitutions.[65] (C) Overall addition of a ligand to a metal ion complex usually requires three-body collisions (or radiative relaxation) to occur. Accordingly, adduct-forming reactions are normally only observed in higher pressure experiments (such as

in the FA) where termolecular kinetics are favorable.[20] A few exceptions to this are known, however.

In one of the early pioneering investigations of gas-phase metal ion chemistry using ICR,[68] Corderman and Beauchamp reported that the nickelocene molecular anion Cp_2Ni^- (Cp = C_5H_5) fails to undergo any detectable reactions in the presence of a large excess of either CO, HCl, NO, HCN, or NH_3. The absence of any ligand substitution or condensation reactions was attributed to the strength of the nickel–cyclopentadienyl bond in the negative ion. A subsequent study of the negative ion chemistry of $CpCo(CO)_2$ provided the first examples of ligand displacement reactions involving anionic metal complexes.[69] Electron impact ionization of $CpCo(CO)_2$ in the ICR produces a molecular anion $CpCo(CO)_2^-$ and a (formally) 17-electron fragment ion $CpCo(CO)^-$ by dissociative electron capture. Both ions were observed to react with NO and PF_3 by CO displacement (eq 19, 20). When a mixture of both NO

$$\begin{aligned} CpCo(CO)_2^- &\xrightarrow{NO} CpCo(NO)^- + 2CO \\ CpCo(CO)_2^- &\xrightarrow{PF_3} CpCo(CO)PF_3^- + CO \\ CpCo(CO)^- &\xrightarrow{NO} CpCo(NO)^- + CO \end{aligned} \quad (19)$$

$$CpCo(CO)^- \xrightarrow{PF_3} CpCo(PF_3)^- + CO \xrightarrow{PF_3} CpCo(PF_3)_2^- \quad (20)$$

and PF_3 was present in the cell, no ligand exchange with either substitution product ion could be observed (eq 21). The primary $CpCo(CO)_{2,1}^-$ ions fail to react with

$$CpCo(NO)^- + PF_3 \not\rightarrow CpCo(PF_3)^- + NO \quad (21)$$

C_2F_4, HCN, ethylene oxide, MeCN, NH_3, NMe_3, and PMe_3. These results were interpreted by Corderman and Beauchamp in terms of the π-acceptor abilities of the various ligands. Here, NO and PF_3 were considered to be stronger π-acceptors than CO, while each of the unreactive molecules listed above is weaker than CO. The suggestion was made that the relative metal–ligand bond strengths that dictate the occurrence or nonoccurrence of substitution in the electron-rich cobalt complex (D[$CpCo^-$–L]) are largely determined by the ability of L to π-backbond to the metal and that the σ-donor ability of L plays a less important role. These conclusions are exactly opposite to those made previously about the metal–ligand bond strengths in the $CpNi^+$ cation (D[$CpNi^+$–L]) which were shown to be mainly determined by the σ-donor ability of L.[65]

Accounts of ligand substitution and addition reactions involving negative metal ions did not appear again until quite recently. McDonald and co-workers used the flowing afterglow method to study the reactions of $Fe(CO)_3^-$ with a variety of small molecules.[45] This reactive 15-electron ion was formed by ionization of $Fe(CO)_5$ using a relatively high emission current (ca. 5 mA) at an immersed EI source. With a total helium pressure of 0.5 Torr in the flow reactor, $Fe(CO)_3^-$ exhibits both addition and CO displacement reactions (eq 22). Addition (eq 22a) was observed with H_2, CO, N_2, $CH_2{=}$

$$Fe(CO)_3^- + X \xrightarrow{a} (CO)_3Fe(X)^- \qquad \xrightarrow{b} (CO)_2Fe(X)^- + CO \qquad \xrightarrow{c} (CO)Fe(X)^- + 2CO \quad (22)$$

$CHCH_3$, and $CH_2{=}C{=}CH_2$; displacement of one CO (eq 22b) occurs with $CH_2{=}C{=}CH_2$ and HC≡CH, and two CO ligands are expelled (eq 22c) from the product of the reaction with CH_3Br. The primary product ion formed with allene, $(CO)_3Fe(C_3H_4)^-$, reacts further to produce $(CO)_2Fe(C_3H_4)_2^-$. On this basis it was proposed that the allene molecules are bonded to iron as (η^2-π)-ligands. A π-ligand structure was also suggested for $(CO)_2Fe(C_2H_2)^-$ wherein the acetylene serves as a four-electron donor. Oxidative insertion structures were proposed for the H_2 adduct $(CO)_3FeH_2^-$ and the CH_3Br condensation product $(CO)Fe(Br)CH_3^-$, corresponding to 17-electron and 13-electron metal ions, respectively. McDonald emphasized the enhanced reactivity of $Fe(CO)_3^-$ by noting that the 17-electron complex $Fe(CO)_4^-$ does not react with any of these neutral substrates under similar conditions. This is understandable, considering that direct association of any of the 2-electron (σ or π) donor ligands with $Fe(CO)_4^-$ would produce a 19-electron intermediate. These results provide the suggestion that associative interchange (I_a) type mechanisms involving 17-electron negative ion (iron) complexes in the gas phase are relatively disfavored.

Wang and Squires investigated ligand substitution and addition reactions involving a pair of isomeric molecular negative ions formed from (η^4-1,3-butadiene)tricarbonyliron ((BUD)$Fe(CO)_3$) and (η^4-trimethylenemethane)tricarbonyliron ((TMM)$Fe(CO)_3$)

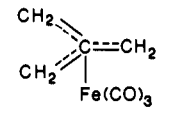

(TMM)$Fe(CO)_3$

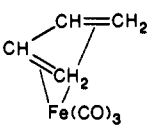

(BUD)$Fe(CO)_3$

by electron capture in a flowing afterglow apparatus.[70] In reactions with the series of π- and σ-donor ligands CO_2, CS_2, SO_2, NO, and CO, the (BUD)$Fe(CO)_3^-$ ion was found to be less reactive than the (TMM)$Fe(CO)_3^-$ ion and to show a greater tendency for displacement of the hydrocarbon ligand instead of CO. For instance, no reaction occurs between (BUD)$Fe(CO)_3^-$ and either CO_2 or CS_2, whereas the (TMM)$Fe(CO)_3^-$ isomer reacts exclusively (albeit slowly) by displacement of a single CO. Both ions react slowly with CO to produce traces of $Fe(CO)_4^-$. In reactions with NO and SO_2, essentially complete displacement of the 1,3-butadiene ligand occurs with (BUD)$Fe(CO)_3^-$ (eq 23). In contrast, the

$$\begin{aligned} (BUD)Fe(CO)_3^- &\xrightarrow{SO_2} \underset{>99\%}{Fe(CO)_3(SO_2)^-} \\ (BUD)Fe(CO)_3^- &\xrightarrow{NO} \\ \underset{96\%}{Fe(CO)_3(NO)^-}&, \underset{4\%}{(BUD)Fe(CO)_2(NO)^-} \end{aligned} \quad (23)$$

hydrocarbon ligand is consistently maintained in the major product ions from (TMM)$Fe(CO)_3^-$ (eq 24).

$$\begin{aligned} (TMM)Fe(CO)_3^- &\xrightarrow{SO_2} \underset{45\%}{Fe(CO)_3(SO_2)^-}, \underset{55\%}{(TMM)Fe(CO)_2(SO_2)^-} \\ (TMM)Fe(CO)_3^- &\xrightarrow{NO} \underset{11\%}{Fe(CO)_3(NO)^-}, \\ \underset{21\%}{(TMM)Fe(CO)_2(NO)^-}&, \underset{68\%}{(TMM)Fe(CO)_3(NO)^-} \end{aligned} \quad (24)$$

These results imply a greater iron–hydrocarbon bond strength in the trimethylenemethane ion compared to that of the butadiene ion. This effect probably arises from the greater stability of 1,3-butadiene compared to trimethylenemethane (or methylenecyclopropane) as a free, neutral species. In terms of the arguments proposed earlier by Corderman and Beauchamp,[69] displacement of the η^2-butadiene ligand by NO, SO_2, and CO is expected since the latter are all stronger π-acceptors than a π-coordinated olefin.[71] While the nature of the bonding between the hydrocarbon ligand and iron in $(TMM)Fe(CO)_3^-$ is not known, the substitution results suggest that it too is less strongly bonded to $Fe(CO)_3^-$ than are NO, SO_2, and CO. For a CO ligand, the estimated bond energy in the negative ion $D[(CO)_3Fe^-–CO]$ is 18 ± 7 kcal/mol (Table III).

An especially interesting example of a negative metal ion ligand substitution reaction was recently reported by McDonald and Chowdhury wherein a large, polydentate organic ligand is displaced by the smallest of all possible ligands, the hydrogen atom.[72] Electron capture by (η^4-1,3-cyclohexadiene)tricarbonyliron in the flowing afterglow yields an abundant molecular ion that, like the butadiene complex shown earlier, most likely exists as a 17-electron η^2-diene complex.[48] Hydrogen atoms that are generated in an H_2 stream passed through a microwave discharge cavity just prior to the flow reactor inlet react with the molecular ion to give three primary products (eq 25). It is apparent that

$$(\eta^2\text{-}1,3\text{-}C_6H_8)Fe(CO)_3^- + H \xrightarrow{75\%} (CO)_3FeH^- + C_6H_8$$
$$\xrightarrow{20\%} (CO)_3Fe^- + C_6H_9$$
$$\xrightarrow{5\%} (C_6H_8)Fe(CO)_2(H)^- + CO \quad (25)$$

Fe–H bond formation in $(CO)_3FeH^-$ and C–H bond formation in C_6H_9 are sufficiently exothermic to induce dissociation of the organic ligand from the metal. The most interesting question here concerns the origin of the hydrogen in $(CO)_3FeH^-$, and McDonald and Chowdhury examined the reaction with D atoms to determine the initial site of attack in the metal ion complex. A primary $(CO)_3FeD^-/(CO)_3FeH^-$ ratio of 2.2 was found, and it was concluded from a consideration of the likely intermediates shown in Scheme I that reaction with H or D atoms occurs principally (or exclusively) by initial formation of the Fe–H(D) bond (lower pathway in Scheme I) as opposed to attack at the hydrocarbon ligand. The lesser amount of $(CO)_3FeH^-$ produced may be derived from reversible rearrangement of excited intermediate 1 to 2 or 3 to 5.

2. Reactions with Dioxygen

Lane, Sallans, and Squires have described the extensive oxidation reactions that occur when certain transition-metal carbonyl anions interact with dioxygen in the gas phase (eq 26). In their preliminary studies,

$$M(CO)_n^- \xrightarrow{O_2} M(CO)_xO_y^- \quad (26)$$

the rates and product distributions for the reactions of $Cr(CO)_5^-$, $Fe(CO)_4^-$, and $Mo(CO)_5^-$ with O_2 were determined with a flowing afterglow apparatus operated at 0.3 Torr (He).[73] Subsequent work has extended the

SCHEME I

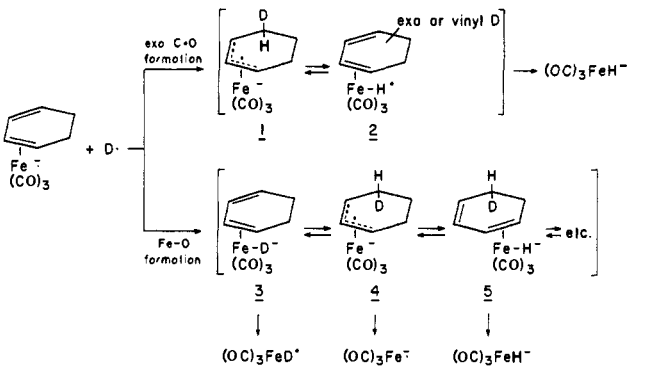

investigation to $V(CO)_5^-$, $W(CO)_5^-$, $Ni(CO)_3^-$, and few other metal anions containing hydrocarbons ligands.[74] These reactions proceed relatively slowly ($k_{meas}/k_{coll} < 0.1$) to yield primary metal ion products in which addition of an O_2 molecule to the metal is accompanied by displacement of one or more CO ligands and CO_2 (eq 27). Table IV presents a summary of the products

$$M(CO)_n^- + O_2 \rightarrow M(CO)_xO_2^- + (n-x)CO$$
$$\rightarrow M(CO)_4O^- + (n-y-1)CO + CO_2 \quad (27)$$

$$n = 3, 4, 5;\ x = 0\text{–}4;\ y = 2$$

observed from reactions of dioxygen with five different 17-electron metal carbonyl ions and one 15-electron ion ($V(CO)_5^-$). With higher O_2 concentrations, all but a few of the primary metal oxide and dioxide products react further to yield relatively unreactive polyoxide ions MO_x^- (x = 2–5). These are listed as the "terminal ions" in the table. While the rates of reaction measured for each of the metal carbonyl anions are similar, the observed product distributions show marked differences. For instance, whereas loss of CO + CO_2 predominates with $Cr(CO)_5^-$, $W(CO)_5^-$, and $Fe(CO)_4^-$, no such product forms at all with $Mo(CO)_5^-$. Moreover, while $Ni(CO)_3^-$ reacts by displacement of a single CO, $V(CO)_5^-$ yields VO_2^- as the major primary product ion by loss of all five CO ligands! The product ion variations can be understood in terms of general periodic trends in metal–oxygen and metal–carbonyl bond strengths. In proceeding to the left along the first row of the transition series, metal–oxygen bond strengths generally increase since higher M–O bond orders can be accommodated.[75] At the same time, metal–carbonyl bond strengths generally decrease due to reduced M(d)–CO(π^*) backbonding.[52,76] Accordingly, metal–oxygen bond formation with the early transition-metal ions will be more exothermic and result in a greater extent of fragmentation of the relatively weakly bonded CO ligands from the product. The differing product distributions for $V(CO)_5^-$ and the group 6 ions compared to $Fe(CO)_4^-$ and $Ni(CO)_3^-$ support this qualitative picture. Metal–oxygen bond strengths also increase down most columns of the transition-series metals,[76] and the greater extent of CO loss in the $W(CO)_5^-$ and $Mo(CO)_5^-$ reactions compared to that in $Cr(CO)_5^-$ parallels this trend.

The radical nature of the initial O_2 reaction mechanism is suggested by the complete lack of reactivity exhibited by the closed-shell, 18-electron ions $Co(CO)_4^-$ and $Mn(CO)_5^-$ (produced from $Co_2(CO)_8$ and $Mn_2(CO)_{10}$, respectively). For the reactive 17-electron radical

SCHEME II

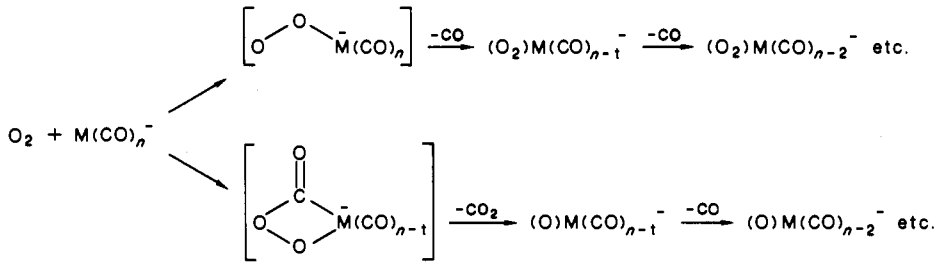

TABLE IV. Reactions of Metal Carbonyl Anions with Dioxygen[a]

$M(CO)_n^-$	primary metal ion products (%)	terminal ions
$Ni(CO)_3^-$	$Ni(CO)_2O_2^-$ (97)	NiO_2^-
	$Ni(CO)O_2^-$ (2)	NiO_3^-
	$Ni(CO)O^-$ (1)	NiO_4^-
$Fe(CO)_4^-$	$Fe(CO)_2O^-$ (75)	FeO_2^-
	$Fe(CO)_3O_2^-$ (15)	FeO_3^-
	$Fe(CO)_3O^-$ (5)	FeO_4^-
	$Fe(CO)_2O^-$ (5)	$Fe(CO)_3O_2^-$
$Cr(CO)_5^-$	$Cr(CO)_3O^-$ (95)	CrO_2^-
	$Cr(CO)_3O_2^-$ (5)	CrO_3^-
		CrO_4^-
		CrO_5^-
		$Cr(CO)_3O_2^-$
$Mo(CO)_5^-$	$Mo(CO)_3O_2^-$ (55)	MoO_3^-
	$Mo(CO)_4O_2^-$ (45)	MoO_4^-
$W(CO)_5^-$	$W(CO)_3O^-$ (56)	WO_2^-
	$W(CO)_3O_2^-$ (20)	WO_3^-
	$W(CO)O_2^-$ (13)	WO_4^-
	$W(CO)_2O_2^-$ (10)	WO_5^-
	$W(CO)_4O_2^-$ (1)	
$V(CO)_5^-$	VO_2^- (43)	VO_3^-
	$V(CO)O_2^-$ (35)	VO_4^-
	$V(CO)_3O_2^-$ (11)	$V(CO)_4O_2^-$
	$V(CO)_3O^-$ (7)	
	$V(CO)_4O_2^-$ (4)	

[a] Taken from ref 73 and ref 74.

anions listed in Table IV, an associative mechanism involving direct attack by $^3O_2$ at the metal followed by CO displacement and/or metallocycle formation can be proposed (Scheme II). Analogous mechanisms have been formulated for the formation of neutral metal carbonyl oxides during photolysis of O_2-doped metal carbonyl matrices at low temperature.[77] The 16-electron $V(CO)_5^-$ ion may accommodate η^2-bonding of O_2 to the metal in the initial adduct, and this may account for the predominance of multiple CO losses rather than loss of CO + CO_2.

A few reactions of O_2 with organometallic anions possessing hydrocarbon ligands were also investigated.[74] The interesting possibility exists with these reactions for oxidation of the organic ligand, in addition to oxidation of the metal and/or CO. Electron impact ionization of $CpMn(CO)_3$ and $CH_3Mn(CO)_5$ in a flowing afterglow produces the 17-electron complexes $CpMn(CO)_2^-$ and $CH_3Mn(CO)_4^-$, respectively, as the major fragment ions. $CpMn(CO)_2^-$ reacts relatively slowly with O_2 to yield $CpMnO_2^-$ as the sole primary product ion (eq 28). At higher O_2 concentrations, MnO_2^-, MnO_3^-, and MnO_4^- grow in at the expense of $CpMnO_2^-$.

$$CpMn(CO)_2^- + O_2 \xrightarrow{-2CO} CpMnO_2^- \xrightarrow{O_2} MnO_2^-, MnO_3^-, MnO_4^- \quad (28)$$

The actual fate of the organic ligand in these secondary oxidations is not known. However, the appearance of MnO_2^- as a product ion from $CpMnO_2^-$ *requires* that the cyclopentadienyl and oxygen neutral fragments be combined in some fashion; otherwise, this particular reaction could not have occurred on thermodynamic grounds. A more extensive primary product distribution results from reaction of O_2 with $CH_3Mn(CO)_4^-$ (eq 29). The remainder of the primary product ions are

$$\begin{aligned} CH_3M(CO)_4^- + O_2 &\xrightarrow{33\%} Mn(CO)_3O^- + (CH_3 + CO_2) \\ &\xrightarrow{30\%} CH_3Mn(CO)O^- + 2CO + CO_2 \\ &\xrightarrow{12\%} CH_3Mn(CO)_2O^- + CO + CO_2 \end{aligned} \quad (29)$$

all produced in <10% relative yield and include $CH_3Mn(CO)_3O_2^-$, $CH_3Mn(CO)_2O_2^-$, $CH_3Mn(CO)_2^-$, MnO^-, and $CH_3CO_2^-$. The appearance of acetate ion is especially interesting since it represents a first example where the organic product of the oxidation reaction maintains the negative charge rather than the metal product. As with $CpMn(CO)_2^-$, the ions MnO_2^-, MnO_3^-, and MnO_4^- dominate the mass spectrum as terminal ions when the O_2 concentration is increased.

Wang and Squires also investigated the reactions of O_2 with the two isomeric ions $(TMM)Fe(CO)_3^-$ and $(BUD)Fe(CO)_3^-$.[70] As in the ligand substitution reaction described in the previous section, the $(BUD)Fe(CO)_3^-$ isomer reacts with O_2 at a slower rate than does $(TMM)Fe(CO)_3^-$ and yields quite different products (eq 30 and 31). The hydrocarbon ligand is maintained in

$$\begin{aligned} (TMM)Fe(CO)_3^- + O_2 &\xrightarrow{66\%} (TMM)FeO_2^- + 3CO \\ &\xrightarrow{23\%} (TMM)FeO^- + 2CO + CO_2 \\ &\xrightarrow{9\%} (TMM)Fe(CO)O^- + CO + CO_2 \\ &\xrightarrow{2\%} FeO^- + (C_4H_6 + 2CO + CO_2) \end{aligned} \quad (30)$$

$$\begin{aligned} (BUD)Fe(CO)_3^- + O_2 &\xrightarrow{40\%} Fe(CO)_2O^- + (C_4H_6 + CO_2) \\ &\xrightarrow{37\%} Fe(CO)_2O_2^- + (C_4H_6 + CO) \\ &\xrightarrow{12\%} Fe(CO)_3O_2^- + C_4H_6 \\ &\xrightarrow{11\%} (BUD)Fe(CO)_3O_2^- \end{aligned} \quad (31)$$

essentially all of the metal oxide product ions from

SCHEME III

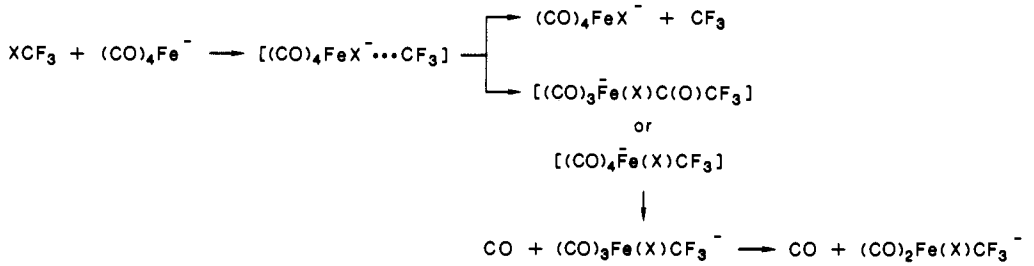

(TMM)$Fe(CO)_3^-$, while it is displaced most of the time as a result of oxidation of (BUD)$Fe(CO)_3^-$. The iron oxide ions that result from (BUD)$Fe(CO)_3^-$ are essentially the same as those derived from $Fe(CO)_4^-$ (Table IV). At higher O_2 concentrations, FeO_2^-, FeO_3^-, and FeO_4^- are produced from both isomers.

3. Oxidative Insertion/Reductive Elimination

Oxidative insertion of a transition metal into σ bonds and the reverse process, reductive elimination, represent two of the most important and pervasive classes of inorganic reaction (eq 32).[78] Countless examples of in-

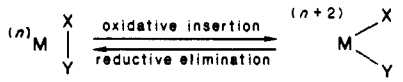

(32)

sertion and elimination reactions involving organometallic species in homogeneous solutions, heterogeneous media, and low-temperature matrices have been reported, and the current picture of these processes has achieved impressive clarity. Electronic structure calculations have made especially significant contributions to the understanding of these reactions in recent years.[79] Insertion–elimination mechanisms are routinely invoked for reactions of atomic and molecular metal cations in the gas phase.[80] Extensive accounts of the mechanisms, thermochemistry, and selectivity of these reactions with saturated and unsaturated hydrocarbons, alkyl halides, alcohols, carbonyl compounds, and other organic molecules are available, and the field has been reviewed recently by Allison.[81]

There are growing numbers of examples of oxidative insertion and reductive elimination type reactions involving gaseous transition-metal negative ions. As was mentioned earlier (section III), atomic metal anions have not yet exhibited this kind of reactivity, at least under the low-pressure conditions of FTMS experiments. However, recent flowing afterglow studies of coordinatively unsaturated metal anion fragments have exposed rich and interesting insertion–elimination reactions with a variety of organic and inorganic substrates.

McDonald and co-workers have described the oxidative insertion reactions of $Fe(CO)_4^-$ with polyhalogenated methanes, XCY_3 (X = I, Br, Cl, Y = F, Cl).[60] With most substrates, the major reaction channel observed is halogen atom abstraction (eq 33). Both

$$(CO)_4Fe^- + XCY \rightarrow (CO)_4FeX^- + CY_3 \quad (33)$$

$$XCY_3 = ICF_3, BrCF_3$$

ICF_3 and $BrCF_3$ also yield lesser amounts of $(CO)_{2,3}Fe(X)(CF_3)^-$ products arising from displacement of one or two CO ligands, and no reaction occurs with CH_3I and $ClCF_3$. A stepwise mechanism was proposed wherein halogen transfer occurs within the ion–molecule collision complex to give an 18-electron $(CO)_4FeX^-$ species that is electrostatically bound to the CF_3 radical (Scheme III). The nascent radical fragment may dissociate from the complex or add to the metal with accompanying CO loss to yield the observed products. The measured rates of reaction show a rough inverse correlation with $D[X-CF_3]$, suggesting that halogen abstraction is rate determining and that the CO displacement channels involve rupture of the $X-CF_3$ bonds.

While $Fe(CO)_4^-$ and other 17-electron metal anions (understandably) do not appear to undergo direct oxidative insertion reactions, metal anion complexes having 16 valence electrons or less have been generated that show extensive insertion chemistry. Recall, for example, the $Fe(CO)_3^-$ ion described earlier.[45] This 15-electron ion yields adducts with a variety of small molecules, including H_2. These products were proposed by McDonald to possess bond-insertion-type structures (eq 34). The consequences of H_2 insertion are espe-

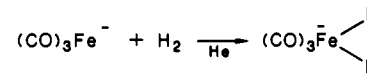

(34)

cially interesting with the 15-electron butadiene complex $(\eta^4\text{-}C_4H_6)Fe(CO)^-$, which was prepared by McDonald and co-workers by EI ionization of $(\eta^4\text{-}C_4H_6)Fe(CO)_3$ with energetic electrons.[82] Termolecular addition of H_2 occurs at 0.55 Torr in a mixed helium/CH_4 buffer (eq 35). Deuterium reacts at a faster overall rate to

$$(\eta^4\text{-}C_4H_6)Fe(CO)^- + H_2 \rightarrow (\eta^4\text{-}C_4H_6)Fe(CO)H_2^- \quad (35)$$

yield an adduct as well as up to four H/D exchanges in the butadiene ligand (eq 36). It was suggested that

$$(C_4H_6)Fe(CO)^- + D_2 \rightarrow (C_4H_{2+x}D_{4-x})Fe(CO)^- \xrightarrow{D_2} (C_4H_{2+x}D_{4-x})Fe(CO)D_2^- \quad x = 0\text{–}4 \quad (36)$$

the occurrence of a maximum of four exchanges shows that only the two terminal methylene groups of the butadiene ligand are involved. A sequential mechanism involving D_2 addition to the metal followed by reversible rearrangement to a π-allyl complex was proposed (Scheme IV). Scrambling of deuterium among the terminal C–H positions followed by reductive elimination of HD or H_2 affects the overall exchange.

McDonald, Chowdhury, and Jones have prepared other multicoordinatively and multielectronically unsaturated transition-metal carbonyl ions in a flowing afterglow with the use of the high emission current EI technique. The reactions of the 14-electron $Mn(CO)_3^-$ ion (from $Mn_2(CO)_{10}$) and the 13-electron $Fe(CO)_2^-$ ion (from $Fe(CO)_5$) with a series of small molecules have been examined.[83] As with $Fe(CO)_3^-$, both ions form

SCHEME IV

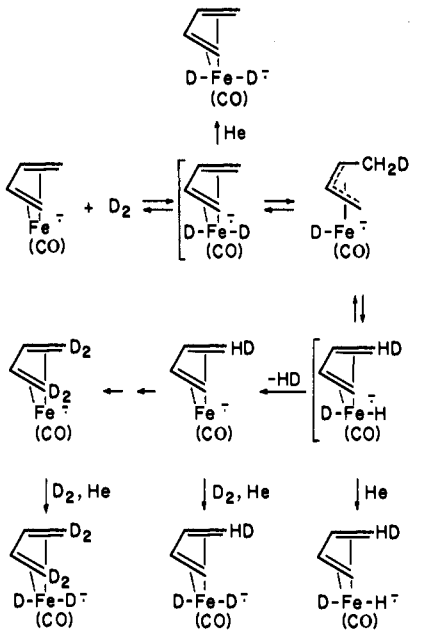

adducts with dihydrogen. The measured reaction efficiencies are identical for H_2 and D_2, as would be expected for termolecular addition reactions where collisional stabilization of the excited intermediate adduct is the rate-determining step. Interesting insertion–elimination reactions were observed with the binary hydrides H_2O, H_2S, NH_3, and PH_3. Both $Fe(CO)_2^-$ and $Mn(CO)_3^-$ react with H_2O by exclusive CO displacement (eq 37a). However, the occurrence of H_2 elimination in secondary H_2O reactions with $Fe(CO)_2^-$ (eq 37b)

$$(CO)_2Fe^- + H_2O \rightarrow (CO)Fe(H)(OH)^- + CO \quad (37a)$$

$$(CO)Fe(H)(OH)^- + H_2O \rightarrow (CO)Fe(OH)_2^- + H_2 \quad (37b)$$

along with the measured rate decrease when D_2O is the reactant (normal kinetic isotope effect) suggests that OH(D) insertion occurs in the primary reaction. This is clearly evident in reactions with H_2S, where H_2 elimination dominates (eq 38 and 39). No primary

$$(CO)_2Fe^- + H_2S \rightarrow (CO)FeS^- + CO + H_2 \quad (38)$$

$$(CO)_3Mn^- + H_2S \xrightarrow{71\%} (CO)_2MnS^- + CO + H_2$$
$$\xrightarrow{29\%} (CO)_3MnS^- + H_2 \quad (39)$$

kinetic isotope effects were found in reactions with D_2S. Analogous reactions were observed for $(CO)_2Fe^-$ with the group 15 hydrides NH_3 and PH_3, i.e., CO displacement and/or H_2 elimination, with the normal primary kinetic isotope effect for NH_3 vs. ND_3, suggesting that oxidative insertion has occurred. The reaction of $(CO)_3Mn^-$ with NH_3 is unique in that an adduct-ion forms as the sole product (eq 40). On the basis

$$(CO)_3Mn^- + NH_3 \xrightarrow[He]{} (CO)_3Mn(NH_3)^- \text{ or } (CO)_3Mn(H)(NH_2)^- \quad (40)$$

of the identical measured rates of reaction for NH_3 and ND_3 and the absence of decarbonylation, it was concluded that the product ion in eq 40 is a simple adduct in which an intact ammonia molecule occupies a metal coordination site as a σ-donor; i.e., N–H insertion has

SCHEME V

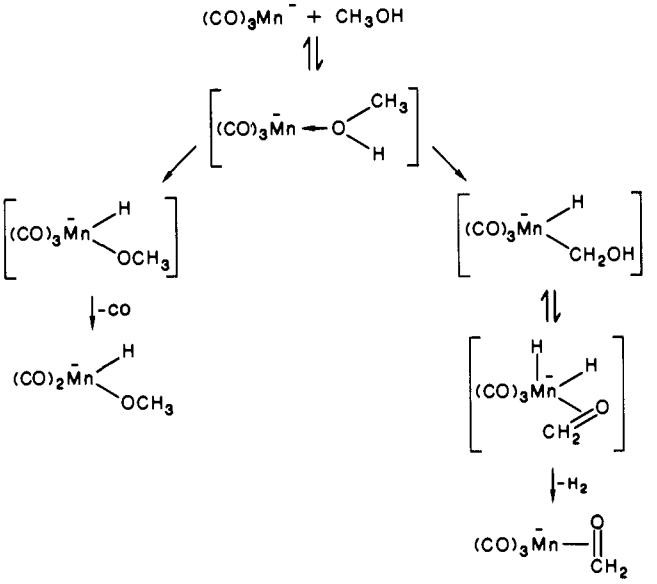

not occurred. However, as noted earlier the rate-determining step for an addition reaction in the gas phase may be collisional stabilization by the bath gas, so the absence of a kinetic isotope effect does not necessarily provide any information about the structure of the adduct.

Kinetic isotope effects were also employed to characterize the mechanism of the reaction of $Mn(CO)_3^-$ with CH_3OH.[85] Two products are produced corresponding to CO displacement and dehydrogenation (eq 41). Exclusive loss of HD occurs in the dehydrogena-

$$Mn(CO)_3^- + CH_3OH \xrightarrow{29\%} (CO)_2Mn(H)(OCH_3)^- + CO$$
$$\xrightarrow{71\%} (CO)_3Mn(H_2CO)^- + H_2 \quad (41)$$

tion channel when either CH_3OD or CD_3OH is used, showing that β-elimination follows oxidative insertion. Analysis of the partial rates for H_2, HD, and D_2 elimination with CH_3OH, CH_3OD, CD_3OH, and CD_3OD led to the conclusion that the initial intermolecular oxidative addition of the H–C and D–C bond to $Mn(CO)_3^-$ is rate limiting for this channel and that intramolecular migration of H or D from oxygen to the metal is fast and does not contribute to the observed isotope effect. Moreover, an isotope ratio $k_{HO}/k_{DO} \simeq 7$ was derived for oxidative insertion into the OH bond. Thus, the two channels in eq 41 arise from distinct intermediates produced by competitive intermolecular insertion into the CH and OH bonds of CH_3OH (Scheme V). Note that in Scheme V these two intermediates are shown to arise from an initial complex involving a coordinate-covalent bond to CH_3OH. While this precursor is not required by the observed results, it is considered likely on the basis of the prevalence of such complexes in solution[66] as well as the earlier proposal regarding the structure of the observed adduct of $(CO)_3Mn^-$ with NH_3. Insertion into the C–O bond to give $(CO)_nMn(CH_3)(OH)^-$ was ruled out on the grounds that the CO displacement product fails to undergo H/D exchange with added D_2O, whereas an analogous product formed from water, $(CO)_2Mn(H)(OH)^-$, which necessarily possesses a hydroxyl ligand, gives a single H/D exchange.

SCHEME VI

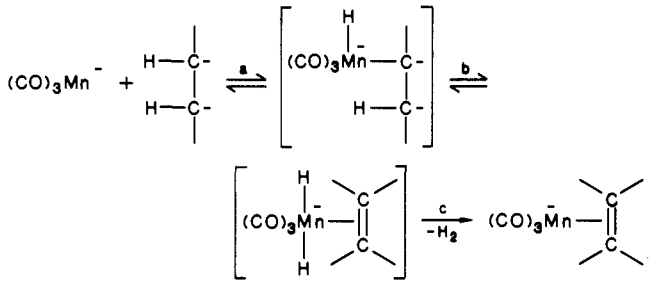

SCHEME VII

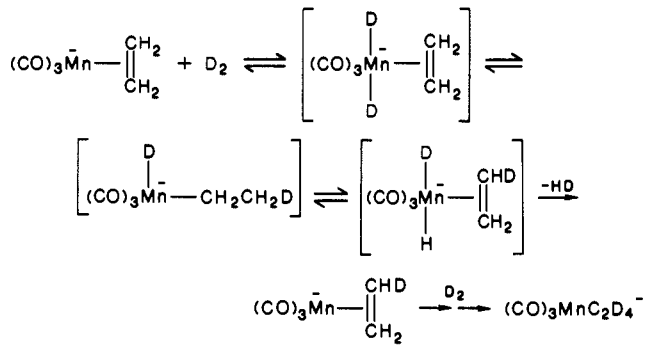

In related studies,[86] the $Mn(CO)_3^-$ ion was found to react with simple alkanes by a C–H insertion β-H_2 elimination mechanism that is common in metal cation reactions[81] (Scheme VI). The dehydrogenation product from reaction with ethane was shown to be the 16-electron π-olefin complex from its further reaction with D_2 where up to four H/D exchanges were observed (Scheme VII). This result also shows that the β-elimination and olefin insertion steps are reversible. With larger alkanes such as propane and isobutane, no H/D exchange occurs with the dehydrogenation products, suggesting that (unreactive) 18-electron hydrido-π-allyl structures are formed by insertion into the allylic CH bonds (eq 42).

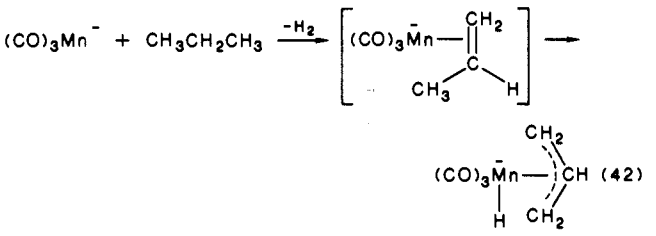

(42)

McDonald and Jones have performed careful rate measurements for the reactions with CH_3CH_3, $CH_3CH_2CH_3$, $(CH_3)_3CH$, and c-C_5H_{10} in order to determine whether any selectivity exists for insertion into primary, secondary, or tertiary C–H bonds.[86] Operating on the assumption that the partial rate for 1° C–H insertion in isobutane is equal to the total rate measured for ethane, they derived the statistically corrected relative rates for intermolecular CH insertion illustrated below:

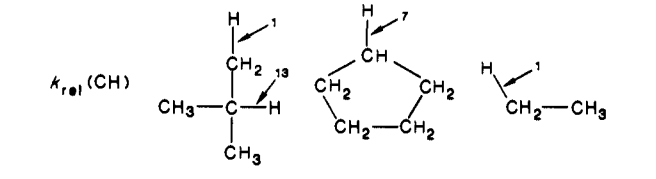

In support of these conclusions, a smaller primary kinetic isotope effect was found for the 1° CH bonds in isobutane, $k_{(CH_3)_3CH}/k_{(CD_3)_3CH} = 1.3$, compared to that for ethane ($k_{C_2H_6}/k_{C_2D_6} = 2.2$). This result requires that 1° CH insertion makes a lesser contribution to the total rate for reaction of $Mn(CO)_3^-$ with isobutane than it does for ethane, viz., 3° CH insertion dominates. The β-elimination step b in Scheme VI was proven to be relatively fast and reversible (and, therefore, not responsible for the overall rate differences among the alkanes) with the results for $CH_3CD_2CH_3$ (eq 43).

$$(CO)_3Mn^- + CH_3CD_2CH_3 \xrightarrow{56\%} (CO)_3Mn(C_3H_5D)^- + HD$$
$$\xrightarrow{44\%} (CO)_3Mn(C_3H_4D_2)^- + H_2 \quad (43)$$

Here, the putative intermediate for the reaction, (6),

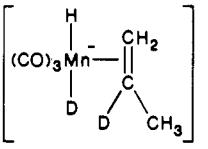

6

formed irrespective of the site of initial CH insertion, could only eliminate HD unless hydrogen scrambling by reversible olefin insertion–β-elimination occurred rapidly compared to the reductive elimination step.

McElvany and Allison have used ICR to investigate the gas-phase reactions of $Fe(CO)_{3,4}^-$, $Cr(CO)_{3,4,5}^-$, $Co(CO)_{2,3}^-$, and $Co(NO)(CO)_{1,2}^-$ with the mono- and bifunctional organic molecules shown below:[87]

$C_nH_{2n+1}Cl$	$C_nH_{2n+1}OH$	$C_nH_{2n+1}NO_2$
$(CH_3)_3CNO_2$	$ClC_nH_{2n}Br$	$ClC_nH_{2n}OH$
	C_4H_9ONO	

For the halides and alcohols n ranged from 1 to 6, and primary nitroalkanes up to $C_4H_9NO_2$ were examined. Extensive tables of the observed product distributions and the presumed ion structures may be found in the original papers.[87] With all substrates, only those metal ions with fewer than 17 valence electrons are reactive; i.e., $Fe(CO)_4^-$, $Cr(CO)_5^-$, and $Co(NO)(CO)_2^-$ do not react. Reactions with n-alkylchlorides were reported to produce three types of products corresponding to CO-ligand substitution (eq 44a), chlorine atom abstraction (eq 44b) and dehydrohalogenation (eq 44c). The occurrence of multiple CO displacements with $Cr(CO)_3^-$ (–3CO), $Fe(CO)_3^-$ (–2CO), and $Co(CO)_2^-$ (–2CO) suggests that C–Cl insertion occurs to produce strong M–Cl bonds. Similar reactions occur with 1,n-bromochloroalkanes along with interesting double-halogen transfers that are accompanied by complete CO loss. The organic fragments in these latter reactions are proposed to be cycloalkanes (or ethylene in the case of $ClCH_2CH_2Br$) which could conceivably form through a bis insertion–reductive elimination mechanism (eq 45). Cyclic ketones were also noted as viable neutral products based

$$M(CO)_n^- + RCl \xrightarrow{a} (RCl)M(CO)_{n-m}^- + mCO$$
$$\xrightarrow{b} ClM(CO)_{n-m}^- + R + mCO$$
$$\xrightarrow{c} (HCl)M(CO)_{n-m}^- + (R\text{–}H) + mCO \quad (44)$$

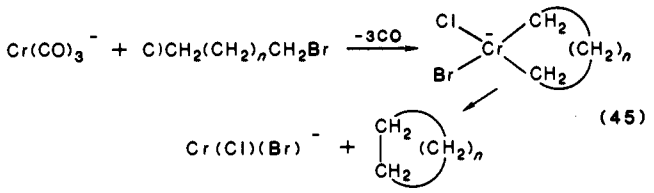

(45)

on thermochemical estimates. As with the $Mn(CO)_3^-$ ion described earlier,[83,85] alcohols react with $Cr(CO)_3^-$, $Fe(CO)_3^-$, $Co(CO)_2^-$, and $Co(NO)(CO)^-$ mainly by dehydrogenation and CO displacement. For alcohols of three carbons or more, bis dehydrogenation with accompanying CO loss was also observed with $Cr(CO)_3^-$ (eq 46). Bifunctional 1,*n*-chloro alcohols react with

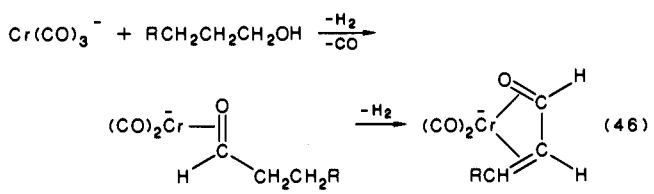

(46)

these same metal ions mainly by chlorine atom transfer and dehydrohalogen reactions that are similar to those shown in eq 44. The $Co(CO)_2^-$ also produces a significant amount of $Co(Cl)(OH)^-$ from reaction with β-chloroethanol, presumably through a tandem C–Cl, C–OH insertion mechanism (eq 47). Interestingly, none of the higher chloro alcohols gave this type of product.

$$Co(CO)_2^- + ClCH_2CH_2OH \xrightarrow{29\%} Co(Cl)(OH)^- + CH_2{=}CH_2 \quad (47)$$

Nitroalkanes and *n*-butyl nitrite react with each of the coordinatively unsaturated metal ions to yield numerous products in relatively low yields. Among the major processes observed with $Fe(CO)_3^-$ and $Co(CO)_2^-$ is a decarboxylation reaction that is reminiscent of the well-known reactions between amine *N*-oxides and metal carbonyls in solution[88] (eq 48). Oxygen abstraction is also observed as a significant channel with each ion (eq 49). Carbonyl ligand substitution domi-

$$Fe(CO)_3^- + CH_3NO_2 \xrightarrow{42\%} Fe(CH_3NO)^- + CO_2 + 2CO \quad (48)$$

$$Co(CO)_2^- + CH_3NO_2 \xrightarrow{32\%} Co(CO)_2O^- + CH_3NO \quad (49)$$

nates the observed reactions between C_4H_7ONO and $Fe(CO)_3^-$, $Co(CO)(NO)^-$, $Co(CO)_3^-$, and $Cr(CO)_4^-$, while HNO abstraction and H_2 elimination were reported to be the major reactions with $Co(CO)_2^-$ and $Cr(CO)_3^-$, respectively.

The presence of a hydride ligand on a coordinatively unsaturated metal anion center can facilitate its reactions with certain hydrogen-containing substrates since an initial oxidative insertion can be rapidly followed by reductive elimination of H_2. This effect is shown by the 15-electron $HFe(CO)_3^-$ ion that has been generated by McDonald and co-workers from the gas-phase reaction between $Fe(CO)_4^-$ and hydrogen atoms[89] (eq 50). The

$$Fe(CO)_4^- + H \xrightarrow{-CO} HFe(CO)_3^- \xrightarrow[[He]]{H_2} H_3Fe(CO)_3^-$$
$$\xrightarrow{-HCO} Fe(CO)_3^- \xrightarrow[[He]]{H_2} H_2Fe(CO)_3^- \quad (50)$$

SCHEME VIII

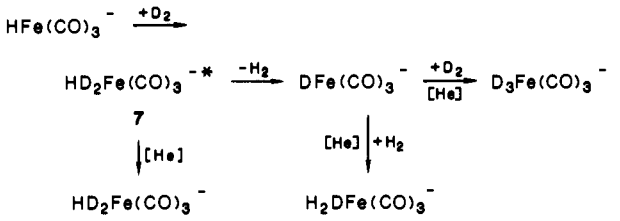

H atoms are generated by flowing H_2 into the reactor through a microwave discharge cavity. Both primary product ions in eq 50 are observed to form adducts with the excess H_2 in the system. When D_2 is allowed to react with this mixture of ions, termolecular addition and H/D exchange occur (eq 51). Analysis of the

$$Fe(CO)_3^-, HFe(CO)_3^- \xrightarrow{D_2} DFe(CO)_3^-, D_2Fe(CO)_3^-, H_2DFe(CO)_3^-, HD_2Fe(CO)_3^-, D_3Fe(CO)_3^- \quad (51)$$

concentration dependence of the product yields shows that all metal ions except $D_2Fe(CO)_3^-$ are derived from $HFe(CO)_3^-$ and that $H_2Fe(CO)_3^-$ is unreactive. An intermediate, energy-rich trihydride complex, formed by reversible oxidative addition of D_2 to $HFe(CO)_3^-$, was proposed to account for the observed scrambling of hydrogen and deuterium (Scheme VIII). An important implication of the occurrence of exchange is that the three hydrogens in the intermediate 7 must become chemically equivalent, perhaps by way of the 18-electron complex 8.

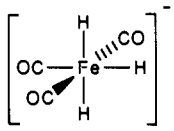

8

Facile H/D exchange with D_2 is also observed with $HCr(CO)_3^-$. Lane and Squires produced this reactive 14-electron metal ion in a flowing afterglow (P = 0.4 Torr) as a product of the reaction between H^- and benzenetricarbonylchromium (section VI) and investigated its reactions with a series of small molecules.[90] Interestingly, while rapid conversion of $HCr(CO)_3^-$ to $DCr(CO)_3^-$ occurs in the presence of D_2, termolecular addition of D_2 (or H_2) to yield $D_3Cr(CO)_3^-$ (or $H_3Cr(CO)_3^-$) does not occur. Note that in the case of $HFe(CO)_3^-$, the H_2 adduct is formally an 18-electron metal ion complex, while a $H_3Cr(CO)_3^-$ complex would contain 16 valence electrons. The complete absence of an observable trihydride in the latter case suggests that the Cr–H bonds are inherently weaker and/or reductive elimination of H_2 is somehow facilitated in this coordinatively unsaturated ion. $HCr(CO)_3^-$ also reacts rapidly with a variety of hydrogen-bearing substrates and Bronsted acids by exclusive addition/H_2 elimination (eq 52). It is instructive to view this process as

$$HCr(CO)_3^- + HX \rightarrow XCr(CO)_3^- + H_2 \qquad X = OH, NH_2, OR \quad (52)$$

a "σ-metathesis" reaction wherein the M–H and H–X bonds are transposed.[91] The reactions of $HCr(CO)_3^-$ with CH_3OH and CH_3OD both proceed at essentially the collision rate; the latter reaction results in exclusive loss of HD (eq 53). This indicates that O–H insertion

$$HCr(CO)_3^- + CH_3OD \rightarrow CH_3OCr(CO)_3^- + HD \quad (53)$$

of the metal, rather than C–H insertion, is the kinetically favored pathway for $HCr(CO)_3^-$. This result is consistent with the conclusions described previously for the $Mn(CO)_3^-$ ion,[85] but indicates that the chromium ion is more oxophilic. Another significant implication of the occurrence of eq 53 is that O–H insertion is irreversible, in accord with the high reaction efficiency determined from the measured kinetics. Otherwise, the reaction with CH_3OD would result in observable H/D exchange in $HCr(CO)_3^-$. Exclusive HD elimination is also observed with D_2O and ND_3.

While $HCr(CO)_3^-$ does not react with alkanes or cycloalkanes, it does react readily with unsaturated hydrocarbons. Insertion–H_2 elimination occurs with propylene and other olefins possessing allylic CH bonds to yield 16-electron π-allyl complexes (eq 54). With

$$CH_2{=}CHCH_3 + HCr(CO)_3^- \longrightarrow \text{[allyl-Cr(CO)}_3^-\text{]} + H_2 \quad (54)$$

isobutylene and cyclic alkenes, addition without H_2 loss occurs Cyclic and acyclic dienes and aromatic compounds such as benzene and toluene react exclusively by addition to yield 18-electron η^4-π-complexes (eq 55).

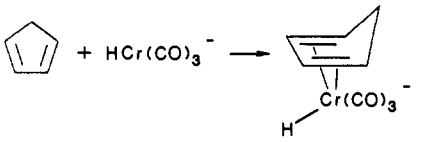

(55)

The results for ethylene, d_4-ethylene, and acetylene suggest that the reactions with olefins are probably more complicated than is implied above. Ethylene reacts relatively slowly by termolecular addition, while C_2D_4 also causes rapid H/D exchange in the metal hydride (eq 56). This latter reaction can occur via

$$HCr(CO)_3^- + CD_2{=}CD_2 \rightarrow DCr(CO)_3^- + CD_2{=}CHD \xrightarrow[\text{[He]}]{} (H)(C_2D_4)Cr(CO)_3^- \quad (56)$$

reversible olefin insertion ("hydrometallation")[92] or vinyl C–H insertion[93] through the appropriate intermediates shown below (eq 57). A relevant finding is

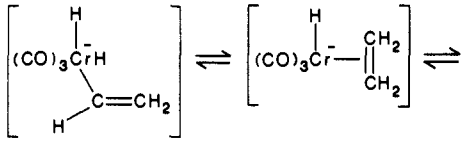

$$[(CO)_3\bar{C}rCH_2CH_3] \quad (57)$$

that acetylene reacts readily to produce both an adduct and the σ-acetylide complex by elimination of H_2 (eq 58). Thus, insertion of the metal into the acetylenic

$$HCr(CO)_3^- + HC{\equiv}CH \rightarrow HC_2Cr(CO)_3^- + H_2 \xrightarrow[\text{[He]}]{} (C_2H_2)(H)Cr(CO)_3^- \quad (58)$$

C–H bond must occur and, by analogy, it may also occur with a vinylic C–H bond. This may appear somewhat surprising since carbon–hydrogen bond insertion selectivity has frequently been rationalized on the basis of homolytic bond strengths in the organic substrates,[94] and acetylenic C–H bonds (D[HC≡C—H] = 125 kcal/mol)[95] are significantly stronger than either vinylic (D[CH_2=CH—H] = 110 kcal/mol)[95] or alkyl C–H bonds (D[CH_3—H] = 105 kcal/mol).[95] However, the heterolytic C–H bond energies exhibit the reverse ordering (D[CH_3^-–H^+] = 416.6 kcal/mol; D[CH_2=CH^-–H^+] = 406 kcal/mol; D[HC≡C^-—H^+] = 375 kcal/mol)[37] and, therefore, an acid–base character to the CH insertion reaction by $HCr(CO)_3^-$ is implied by these results.

It is generally clear from the foregoing material that negative transition-metal ions can be quite reactive in insertion–elimination reactions, oxidations and, to a limited extent, ligand substitutions. This is especially so in cases where the metal possesses fewer than 16 electrons in its coordination sphere and/or a 1-electron donor ligand which may become involved in reductive elimination of a stable molecule following the primary reaction with the substrate. A systematic evaluation of the effects of successive coordinative unsaturation in a series of metal carbonyl negative ions, $M(CO)_n^-$ (n = 0, 1, 2, ...), on the kinetics and mechanisms of gas-phase reactions involving a single substrate would be particularly valuable for illustrating influence of electronic and geometric structure on reactivity. Moreover, in view of the enhanced reactivity shown by $HCr(CO)_3^-$ and $HFe(CO)_3^-$, it seems likely that diatomic metal hydride anions, MH^-, will exhibit extensive insertion–elimination chemistry, perhaps even with alkanes.

V. Metal Cluster Negative Ions

Early on in studies of the gas-phase negative ion chemistry of volatile transition-metal carbonyls, the "self-condensation" reactions between EI-derived metal fragment ions and their precursor complexes were discovered. The first examples of these interesting cluster-forming reactions were reported in 1973 by Dunbar, Ennever, and Fackler, who used an ICR with total ion current monitoring to demonstrate the high-mass capabilities of the technique.[96] The negative ion–molecule reactions shown in eq 59–62 were identified with double-resonance ejection experiments. The likelihood of multiple metal–metal bonds in the presumably paramagnetic dinuclear product ions was suggested by the authors since analogous 18-electron anions such as $Ni_2(CO)_6^{2-}$ were well-known multiply bonded species in solution. Subsequent ICR studies by both Brauman[97] and Beauchamp[98] of the negative ions derived from $Fe(CO)_5$ reaffirmed eq 60 as the principle clustering reaction, as well as the apparent "non-reactivity" of $Fe(CO)_4^-$ toward further condensation noted earlier by Dunbar.

$$Ni(CO)_3^- + Ni(CO)_4 \rightarrow Ni_2(CO)_6^- + CO \quad (59)$$

$$Fe(CO)_3^- + Fe(CO)_5 \rightarrow Fe_2(CO)_6^- + 2CO \quad (60)$$

$$Cr(CO)_4^- + Cr(CO)_6 \rightarrow Cr_2(CO)_6^- + 2CO \quad (61)$$

$$Cr(CO)_3^- + Cr(CO)_6 \rightarrow Cr_2(CO)_6^- + 3CO \quad (62)$$

Corderman and Beauchamp discovered a similar reaction occurring in ionized $CpCo(CO)_2$.[69] While the molecular anion $CpCo(CO)_2^-$ is unreactive, the mono-

carbonyl ion reacts relatively rapidly with excess neutral precursor to yield a dinuclear cluster ion (eq 63). This

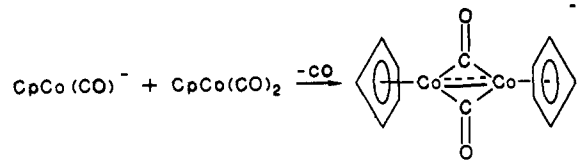

(63)

product was assigned the symmetrical CO-bridging structure shown below in analogy with the known dimer anion which has been prepared in solution and structurally characterized. Partial Co/Co double-bond character is suggested by both MO calculations[99] and the measured ESR spectrum[100] for this paramagnetic complex.

The most detailed characterization and analysis of negative ion clustering reactions in $Fe(CO)_5$ was described quite recently. With use of a frequency-swept ICR spectrometer and multiple resonance techniques for establishing product ion precursors, Wronka and Ridge systematically dissected the complex sequence of condensation reactions occurring in ionized $Fe(CO)_5$ which eventually leads to negative cluster ions containing up to five iron atoms.[101,102] Relative rates of reaction of the primary reactant ions $Fe(CO)_3^-$ and $Fe(CO)_4^-$ and intermediate dinuclear, trinuclear, and tetranuclear ions with $Fe(CO)_5$ were also evaluated. Equation 64–68 summarize the major reactions that

$$Fe(CO)_2^- \xrightarrow[-2CO]{Fe(CO)_5} Fe_2(CO)_5^- \quad (64)$$

$$Fe(CO)_3^- \xrightarrow[-2CO]{Fe(CO)_5} Fe_2(CO)_6^- \quad (65)$$

$$Fe(CO)_4^- \xrightarrow[-CO]{Fe(CO)_5} Fe_2(CO)_8^- \quad (66)$$

$$Fe_2(CO)_5^- \xrightarrow[-CO]{Fe(CO)_5} Fe_3(CO)_9^- \xrightarrow[-2CO]{Fe(CO)_5} Fe_4(CO)_{12}^- \quad (67)$$

$$Fe_2(CO)_6^- \xrightarrow[-CO]{Fe(CO)_5} Fe_3(CO)_{10}^- \xrightarrow[-2CO]{Fe(CO)_5} Fe_4(CO)_{13}^- \quad (68)$$

were identified wherein each condensation step is accompanied by expulsion of one or two CO ligands from the product metal ions. It is noteworthy that the $Fe(CO)_4^-$ was also observed to react (albeit slowly), in contrast to several earlier reports in which it was claimed to be inert.[96-98]

The clustering kinetics exposed an interesting correlation between relative rate of condensation with $Fe(CO)_5$ and the degree of coordinative unsaturation in the reactant metal ions. This latter quantity is evaluated from the electron deficiency per iron atom as given by the expression below (eq 69), where N is the

$$\text{electron deficiency} = [(N \times 18) - (\text{total valence electrons})]/N \quad (69)$$

number of iron atoms in the reactant metal ion, and the number of valence electrons is deduced from assumed structures and metal–metal bond orders.[102] Figure 6 shows a plot of the log of the relative rate constants for reaction of $Fe_n(CO)_m^-$ ions vs. electron deficiency. The key assumptions made by Wronka and Ridge were that each of the dinuclear cluster ions except $Fe_2(CO)_8^-$ possesses a double bond between iron atoms and the

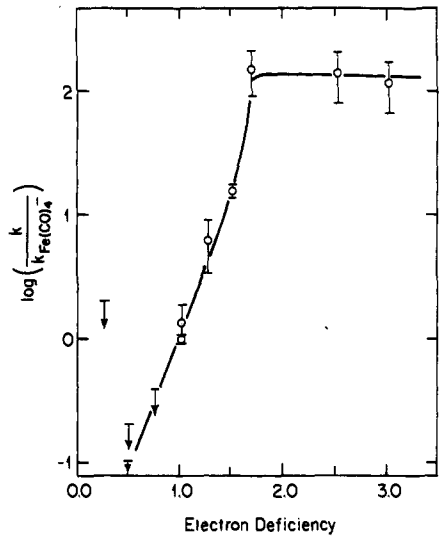

Figure 6. Relative rate constants for reaction of $Fe_n(CO)_m^-$ ions vs. electron deficiency assuming $Fe_2(CO)_m^-$ species have double metal–metal bonds where m = 5, 6, and 7. Reprinted with permission from ref 102. Copyright 1984 American Chemical Society.

triiron and tetrairon clusters involve only single Fe–Fe bonds in triangular and tetrahedral metal frameworks, respectively. These assumptions are reasonable in view of the structures known for iron carbonyl clusters in solution. The smooth decrease in relative rate constants for metal ions with electron deficiencies <1.5, and an approximately constant value for ions with greater deficiencies have a straightforward interpretation. Reactivity is largely predicated on the availability of an open 2-electron coordination site on a metal atom; cluster ions with electron deficiencies of 2 or greater per iron atom should react rapidly with $Fe(CO)_5$ at or near the ion–molecule collision limiting rate. Those metal ions with lesser electron deficiencies must undergo a ligand rearrangement in order to open up a 2-electron vacancy and, therefore, their rate of reaction will be decreased. Wronka and Ridge showed that alternate assignments of Fe–Fe bond orders in calculating electron deficiencies led to irregular behavior in plots like Figure 6. This circumstantial evidence for double bonds in the dimer ions seems compelling. Indeed, the smooth correlation obtained with relative rates for all reactive cluster ions strongly suggests that symmetrical structures are present; otherwise, the *average* values for electron deficiency (per iron atom) would not fit the data.

The above conclusions for the $Fe_n(CO)_m^-$ ($n \geq 2$, $m \geq 6$) ions may not be entirely general, however. As noted earlier in section III, several dinuclear cluster ions were formed from reactions between atomic metal anions and their parent neutral carbonyl complexes which exhibited CID behavior that was suggestive of unusual structures.[31] In particular, the $Cr_2(CO)_5^-$ ion (from eq 4) fragments by loss of a Cr atom when collisionally activated. This is a result more consistent with an unsymmetrical structure involving a bare (or nearly bare) chromium atom ligand as opposed to a complex with equal sharing of electron deficiency between the metals. Moreover, when larger dichromium ions formed through condensation reactions between $Cr(CO)_6$ and other $Cr(CO)_n^-$ fragments are subjected to CID, CO loss occurs sequentially until the $Cr_2(CO)_5^-$ complex is ob-

tained which, again, undergoes exclusive loss of Cr (eq 70).[103] Thus, the same "unusual" structure for a di-

$$Cr(CO)_4^- + Cr(CO)_6 \xrightarrow{-2CO} Cr_2(CO)_8^- \xrightarrow[-3CO]{CID} Cr_2(CO)_5^- \xrightarrow[-Cr]{CID} Cr(CO)_5^- \quad (70)$$

chromium cluster ion is probably achieved after CO ligands are removed from a more saturated complex. This is evidently also the case with diiron cluster ions since CID with $Fe_2(CO)_6^-$ formed by eq 65 in the FTMS yields only CO loss as the lowest energy decomposition until $Fe_2(CO)_4^-$ is produced; subsequently, an Fe atom is lost to yield $Fe(CO)_4^-$ (eq 71).[103] Therefore, it seems

$$Fe(CO)_3^- + Fe(CO)_5 \xrightarrow{-2CO} Fe_2(CO)_6^- \xrightarrow[-2CO]{CID} Fe_2(CO)_4^- \xrightarrow[-Fe]{CID} Fe(CO)_5^- \quad (71)$$

that when a very high degree of coordinative unsaturation is present in a metal carbonyl cluster ion, equal sharing of CO ligands does not occur and one metal center achieves greater saturation at the expense of the other. This interesting phenomenon probably depends on the metal, however, since divanadium cluster ions show only sequential CO loss from CID (eq 9) and, therefore, approximately symmetrical structures are likely to exist throughout the overall decomposition to form V_2^-.

While useful new information about the physical properties and electronic structures of negative metal cluster ions has recently become available from photoelectron measurements,[104] very little is known about the reactions of these species other than self-condensation. Because of their high electron binding energies and extensive charge delocalization, negative metal cluster ions are expected to be thermodynamically weak bases and kinetically poor nucleophiles. Ligand substitution reactions and insertion–elimination chemistry may be facilitated by the presence of multiple metal centers, however, and future studies along these lines would be most interesting. In the one reactivity study published to date, Meckstroth and Ridge examined the reactions of $M_2(CO)_9^-$ (M = Mn, Re) ions with a series of Bronsted acids in an attempt to determine their proton affinities.[46] The dinuclear ions were generated from EI ionization of the series of congeneric complexes $Mn_2(CO)_{10}$, $MnRe(CO)_{10}$, and $Re_2(CO)_{10}$. Neither HCl nor other (weaker) acids were found to protonate any of these cluster ions, setting an upper limit to their proton affinities of 333 kcal/mol.

VI. Reactions of Negative Ions with Neutral Transition-Metal Compounds

Current efforts to investigate reactions involving free negative ions and transition-metal compounds in the gas phase have been inspired, in part, by recognition of the important impact recent gas-phase ion experiments have had on our present understanding of nucleophilic addition and substitution reactions involving organic substrates.[105] Unfortunately, there exist several practical limitations on studies of this type of ion–molecule reaction such as the requirement for high volatility and good thermal stability in the neutral transition-metal reagent—qualities that significantly reduce the number of compounds which may be investigated. Moreover, in many types of instruments ionization of the metal reagent by stray electrons may yield abundant negative metal ions that can severely hamper studies of the desired ion–molecule reaction. However, the more than 20 papers that have appeared on this subject over the past two decades have already exposed some instructive general trends as well as several interesting departures from the behavior of the corresponding reactions in solution.

The first deliberate attempt to examine the gas-phase reactions of independently generated negative ions with a neutral transition-metal complex was reported by Foster and Beauchamp in 1971.[106] The negative ions F^-, $CH_3CH_2O^-$, CN^-, and Cl^-, formed by dissociative electron capture from appropriate precursors, were allowed to react with $Fe(CO)_5$ at relatively low pressure in an ICR.[98] Only F^- and $CH_3CH_2O^-$ were observed to react (eq 72 and 73), and it was noted at the time that

$$F^- + Fe(CO)_5 \rightarrow Fe(CO)_3(F)^- \quad (72)$$

$$CH_3CH_2O^- + Fe(CO)_5 \rightarrow Fe(CO)_3(OCH_2CH_3)^- + 2CO \quad (73)$$

this was probably a reflection of the fact that CN^- and Cl^- are much weaker bases.[37] The metal ion products of eq 72 and 73 were presumed to be four-coordinate, 16-electron complexes. Similar conclusions were reported later by Corderman and Beauchamp in an ICR investigation of the negative ion chemistry of $CpCo(CO)_2$.[69] Of the six negative ions examined in this study, CD_3O^-, F^-, CN^-, NO_2^-, Cl^-, and I^-, again only the stronger bases F^- and CD_3O^- were observed to react (eq 74 and 75). Substituted even-electron cyclo-

$$F^- + CpCo(CO)_2 \xrightarrow{68\%} CpCo(CO)F^- + CO \qquad \xrightarrow{32\%} CpCo(F)^- + 2CO \quad (74)$$

$$CD_3O^- + CpCo(CO)_2 \xrightarrow{84\%} CpCo(CO)(OCD_3)^- + CO \qquad \xrightarrow{8\%} CpCo(OCD_3)^- + CO \qquad \xrightarrow{8\%} CpCo(CO)_2(OCD_3)^- \quad (75)$$

pentadienyl–cobalt structures $CpCo(CO)_nX^-$ (n = 0, 1, 2) were suggested for the products, corresponding to 16- and 18-electron complexes for n = 0 and n = 1, respectively. The adduct observed with CD_3O^- is unusual and is likely to involve addition of the nucleophile at either the hydrocarbon or a carbonyl ligand since direct addition at the metal would produce a η^3-cyclopentadienyl structure.[107]

Hehre and Bartmess recently described gas-phase acidity measurements for mixed chromium arenes $ArCr(C_6F_6)$ (Ar = $C_6H_5CH_3$, m-$C_6H_4(CH_3)_2$, and p-$C_6H_4(CH_3)_2$).[108] Proton-transfer equilibria were established in an ICR between the chromium arenes and a series of amines, thiols, and their conjugate base anions (eq 76). No reactions other than proton transfer were

$$(CH_3C_6H_5)Cr(C_6F_6) + n\text{-}PrS^- \rightleftharpoons (CH_2C_6H_5)Cr(C_6F_6)^- + n\text{-}PrSH \quad (76)$$

reported, and the abstracted protons were assumed to be the benzylic ones by analogy with results from studies of these complexes in solution. The measured

TABLE V. Gas-Phase Negative Ion Reactions of $Fe(CO)_5$, 0.4 Torr[a]

anion (X^-)	PA[b]	primary CO expulsion products[c] $(CO)_3FeX^-$	$(CO)_4FeX^-$	$(CO)_4FeC(O)X^-$	other products
NH_2^-	403.6	+			
H^-	400.4	+	+		
$C_6H_5^-$	398.8	+	+		
$CH_2{=}CHCH_2^-$	391.3		+	+	$(CO)_4Fe^-$
OH^-	390.7	+			
CH_3O^-	381.4	+			$(CO)_4FeCHO^-$
$PhCH_2^-$	379.2	+	+	+	
$CH_3CH_2O^-$	376.1	+			$(CO)_4FeCHO^-$
HC_2^-	375.4	+	+	+	
CH_2CN^-	372.1	+	+	+	
F^-	371.3	+	+	+	
$CH_3C(O)CH_2^-$	368.8			+	
$CF_3CH_2O^-$	364.4	+			
HS^-	353.5			+	
HCO_2^-	345.2			+	$(CO)_4FeH^-$, $(CO)_4FeCHO^-$
N_3^-	344.6				$(CO)_2FeNCO^-$, $(CO)_3FeNCO^-$
Cl^-	333.4			+	

[a] Taken from ref 125. [b] Proton affinity in units of kcal/mol, ref 37. [c] Plus sign indicates appearance of metal ion as a primary product.

acidity enhancement in the chromium arenes relative to the uncomplexed hydrocarbons (22–23 kcal/mol) was found to be comparable to the acidity enhancing effect accompanying para-NO_2 and para-CN substitution in toluene, in accord with the acidity enhancement noted in solution. An MO analysis of the charge distribution in $(CH_3C_6H_5)Cr(CO)_3$ and its deprotonated form showed that very little of the excess negative charge in the conjugate base is delocalized into the $Cr(CO)_3$ fragment, suggesting that the metal complexes incorporate true benzylic-like anions.

Sidorov and co-workers have used Knudsen cell mass spectrometry to investigate fluoride ion addition (eq 77)

$$MF_n + F^- \rightleftharpoons MF_{n+1}^- \quad (77)$$

$$MF_n + M'F_{m+1}^- \rightleftharpoons MF_{n+1}^- + M'F_m \quad (78)$$

and fluoride-ion-transfer reactions (eq 78) occurring in the saturated, high-temperature vapor of a series of transition-metal polyfluorides.[24,25] Direct fluoride addition/dissociation equilibria (eq 77) could be assayed at 1000–1200 K for MF_n = HfF_4,[109] UF_4,[110] and ScF_3,[111] while fluoride-transfer equilibria (eq 78) were analyzed at 900–1200 K for the binary metal fluoride systems $MF_n/M'F_m$ = HfF_4/AlF_3,[109] UF_4/UF_5,[110] FeF_2/AlF_3,[112] FeF_3/AlF_3,[112] ScF_3/AlF_3,[113] ZrF_4/AlF_3,[114] MnF_3/AlF_3,[115] MnF_3/MnF_4,[115] MnF_4/PtF_4,[115] NiF_3/AlF_3,[116] RhF_3/FeF_3,[26] RhF_3/MnF_3,[26] AuF_3/MnF_3,[117] $MoF_3/UF_4/Ni$,[118] and VF_3/MnF_3.[119] From analysis of the temperature dependence of the various equilibria listed above and a knowledge of the absolute fluoride ion binding energy for AlF_3 ($D[AlF_3{-}F^-]$ = 120 ± 2.0 kcal/mol),[24] an extensive compilation of new fluoride affinities, metal polyfluoride ion heats of formation, and electron affinities was developed. Electron-transfer reactions also may be examined with this technique. For example, the equilibrium shown in eq 79 was identified in the vapor

$$PtF_4 + PtF_6^- \rightleftharpoons PtF_4^- + PtF_6 \quad (79)$$

over a MnF_3–MnF_2–Pt mixture and was used to determine the electron affinity of PtF_6 to be 8.0 ± 0.3 eV—a value which, at the time, was noted as being the highest EA known among all inorganic molecules.[120]

ICR techniques are also amenable to the study of fluoride-ion- and electron-transfer reactions of transition-metal polyfluorides, albeit only the most volatile ones since the ICR is normally operated at (or near) room temperature. George and Beauchamp investigated the gas-phase ion–molecule reactions of WF_6 with a variety of potential fluoride- and electron-donor anions.[121] The fluoride ion itself reacts by two pathways (eq 80), while Cl^- does not appear to possess an exothermic channel. Accordingly, $EA(WF_6)$ was bracketed to be between that of F and Cl, or 3.5 ± 0.1 eV. Fluoride transfer to WF_6 was observed from both SF_6^- and SF_5^- (from EI on SF_6), while fluoride abstraction from WF_7^- was observed to occur with BF_3, thereby establishing $D[SF_4{-}F^-]$ = 68 kcal/mol < $D[WF_6{-}F^-]$ < $D[BF_3{-}F^-]$ = 71 kcal/mol.

$$F^- + WF_6 \rightarrow WF_6^- + F$$
$$\rightarrow WF_7^- \quad (80)$$

Gregor and co-workers have recently discussed the analytical utility of Cl^- attachment to organometallic complexes in negative chemical ionization (NCI) sources.[122] A series of zinc(II) β-keto enolates were examined under NCI conditions with a CF_2Cl_2 reagent gas, and abundant M + Cl^- ions were observed.[123] Attachment of the chloride nucleophile was assumed to occur directly at the metal. Chloride ion attachment to $PtCl_2(PEt_3)_2$ under NCI conditions was also recently reported by Turco and Traldi.[124] Considering the increasing number of NCI reagent ions which are now finding useful analytical applications (e.g., OH^-, O_2^-, F^-, NH_2^-, etc.),[4] the potential for future developments in the analyses of organometallic compounds in this way appears excellent.

Lane, Sallans, and Squires have provided extensive accounts of the kinetics, mechanisms, and thermochemistry for reactions of $Fe(CO)_5$ with bare and partially solvated negative ions.[125–129] At the 0.3–0.8-Torr (He) pressures employed in these flowing afterglow experiments, $Fe(CO)_5$ exhibits somewhat different reactivity than was observed previously in the ICR in that most all common types of negative ions react by one or more of the channels shown in eq 81, as well as by electron transfer, ion-transfer or other condensation-type reactions.[125] Table V presents a summary listing of the products observed from several of these reactions. In general, it was found that strongly basic, localized

$$X^- + Fe(CO)_5 \xrightarrow{a} (CO)_3FeX^- + 2CO$$
$$\xrightarrow{b} (CO)_4FeX^- + CO$$
$$\xrightarrow[[He]]{c} (CO)_4FeC(O)X^- \quad (81)$$

nucleophiles such as OH^-, NH_2^-, and most alkoxide ions react mainly or exclusively via path 81a to yield tricarbonyliron products (e.g., eq 82). These reactions

$$NH_2^- + Fe(CO)_5 \rightarrow (CO)_3FeNH_2^- + 2CO \quad (82)$$

were found to proceed with rates at or near the ion–molecule collision limiting values. Other strongly basic anions that do not possess a heteroatom at the nucleophilic site also appeared to react rapidly, but with a lesser extent of CO expulsion from the metal ion products. For example, hydride ion (PA = 400.4 kcal/mol)[37] and phenide ion (PA = 399 kcal/mol)[37] both react to produce tricarbonyl- and tetracarbonyliron products (eq 83). Allyl anion (PA = 391.3 kcal/mol)[37]

$$C_6H_5^- + Fe(CO)_5 \rightarrow (CO)_3Fe(C_6H_5)^- + 2CO$$
$$\rightarrow (CO)_4Fe(C_6H_5)^- + CO \quad (83)$$

yields an adduct, a monodecarbonylation product, and the dissociative charge-transfer product $Fe(CO)_4^-$ (eq 84), while benzyl anion $PhCH_2^-$ and acetonitrile anion

$$CH_2{=}CHCH_2^- + Fe(CO)_5 \xrightarrow{64\%}$$
$$Fe(CO)_4^- + CO + C_3H_5$$
$$\xrightarrow{25\%} (CO)_4FeC(O)C_3H_5^-$$
$$\xrightarrow{11\%}$$
$$(CO)_4Fe(C_3H_5)^- + CO \quad (84)$$

CH_2CN^- produce all three types of products shown in eq 81. The primary tricarbonyliron products were observed to undergo secondary clustering reactions with $Fe(CO)_5$ to yield diiron complexes from which 0, 1, or 2 CO ligands are expelled (eq 85).

$$X^- \xrightarrow[-2CO]{Fe(CO)_5} (CO)_3FeX^- \xrightarrow{Fe(CO)_5}$$
$$Fe_2(CO)_n(X)^- \quad n = 6\text{–}8 \quad (85)$$

The more weakly basic nucleophiles such as enolate ions, halide ions, thiolates, and carboxylates react somewhat more slowly by exclusive (termolecular) addition. This may explain, in part, why the weaker base anions examined previously by Foster and Beauchamp[98] (Cl^-, CN^-) were found to be unreactive, since at the reduced pressures in the ICR (10^{-6} Torr), termolecular addition reactions are usually too slow to be observed.

The general mechanism shown in Scheme IX was proposed for the addition–decarbonylation reactions wherein attack by the nucleophilic anion at a carbonyl ligand is followed by loss of CO from the metal, migratory deinsertion of the group X, and a second CO expulsion to yield the tricarbonyliron product. The observed pressure dependence for certain of the product distributions listed in Table V could be satisfactorily predicted from kinetic models derived from this mechanism.

The thermochemistry of negative ion binding to $Fe(CO)_5$ was shown to play an important role in determining the final product distributions for eq 81. A series of these binding energies, $D[(CO)_4FeCO–X^-]$, were independently determined from anion-transfer equilibrium measurements and relative anion affinity bracketing experiments.[63] A summary of these results is shown in Table VI. Of particular interest in these data are the results for H^-, since the corresponding negative ion adduct is a formyl anion complex of the type that is believed to play an important part in homogeneously catalyzed CO reduction chemistry. The hydride affinity (HA) of $Fe(CO)_5$ and the associated heat of formation of $(CO)_4FeCHO^-$ (9) were estimated[126]

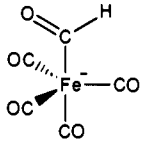

9

from the occurrence of H^- transfer to $Fe(CO)_5$ from a series of reference hydride donor anions such as HCO_2^- ($HA(CO_2)$ = 51.6 kcal/mol), $PhCHCH_3^-$ ($HA(PhCH{=}CH_2)$ = 50.4 kcal/mol), and $(CH_3)_2CCN^-$ ($HA(CH_2{=}C(CH_3)CN)$ = 56.1 kcal/mol) (e.g., eq 86). A final value

$$HCO_2^- + Fe(CO)_5 \rightarrow CO_2 + (CO)_4FeCHO^- \quad (86)$$

for $HA(Fe(CO)_5)$ = 56.1 ± 4.0 kcal/mol was derived, corresponding to $\Delta H_f[(CO)_4FeCHO^-,g]$ = −194.4 ± 4.3 kcal/mol.

The negative ion binding energies of $Fe(CO)_5$ listed in Table VI were found to exhibit linear correlations with the proton affinities, $PA(X^-)$, and the acetyl cation affinities, $(D[CH_3CO^+–X^-])$, of the negative ions (e.g., eq 15).[63] From the anion affinities determined with eq

SCHEME IX

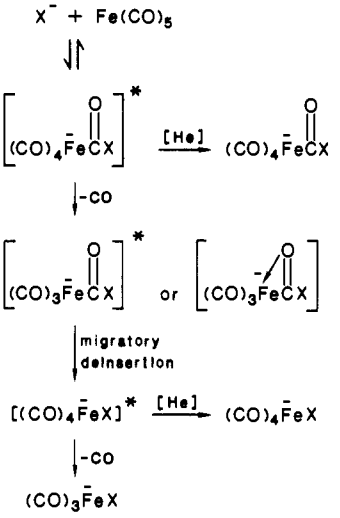

TABLE VI. Experimentally Determined Negative Ion Binding Energies of $Fe(CO)_5$, kcal/mol[a]

X^-	$D[(CO)_4FeCO–X^-]$	X^-	$D[(CO)_4FeCO–X^-]$
H^-	56.1 ± 4	F^-	40.9 ± 3
OH^-	53.1 ≤ x ≤ 60.3	$CF_3CH_2O^-$	≥34.0
MeO^-	39.1 ≤ x ≤ 51.0	MeS^-	≥28.6
EtO^-	≤45.7	HS^-	≥23.1
n-PrO^-	≤44.3	$CH_3CO_2^-$	≤29.5
n-BuO^-	≤43.6	Cl^-	13.9 ± 3
t-BuO^-	≤42.9		

[a] Taken from ref 63.

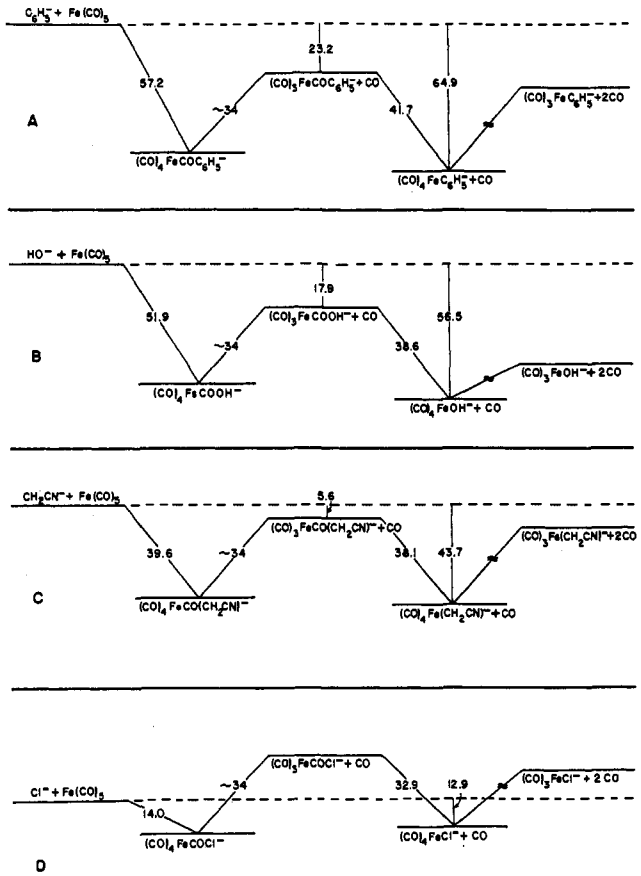

Figure 7. Energy profiles for the gas-phase condensation reactions between $Fe(CO)_5$ and (A) phenide ion, (B) hydroxide ion, (C) acetonitrile anion, and (D) chloride ion. Energies in units of kcal/mol. Reprinted with permission from ref 125. Copyright 1986 American Chemical Society.

15 and other estimates of the energetics for the separate steps of the mechanism shown in Scheme IX, semiquantitative energy profiles for the reactions of negative ions with $Fe(CO)_5$ could be derived, as illustrated in Figure 7. It was concluded that decarbonylation will accompany nucleophilic addition of negative ions which possess $Fe(CO)_5$ binding energies greater than ca. 34 kcal/mol.

The dramatic influence of partial solvation of the anion reactants on the outcome of reaction with $Fe(CO)_5$ was subsequently demonstrated in an investigation[127] of negative ion clusters such as $OH(H_2O)_n^-$ (n = 1–4), $RO(ROH)_n^-$ (n = 1–3), $NH_2(NH_3)^-$, $HS(H_2S)_n^-$ (n = 1, 2), and $CH_3CO_2(CH_3CO_2H)_n^-$ (n = 1, 2). With few exceptions, most all solvated anion reactants examined were found to react rapidly with $Fe(CO)_5$ to yield exclusively the corresponding tetracarbonyliron acyl anion products by complete displacement of the solvent molecules (eq 87). Rate measurements were

$$X(XH)_n^- + Fe(CO)_5 \rightarrow (CO)_4FeC(O)X^- + nXH \quad (87)$$

reported for each reaction, and the trends in the kinetics were discussed. A mechanism was proposed (Scheme X) wherein transfer of the negative ion nucleophile from its solvent shell during a collision with $Fe(CO)_5$ releases sufficient internal energy into the reactive complex to cause expulsion of all of the relatively weakly associated solvent molecules. From an analysis of the thermochemistry for the solvated ion reactions it was determined that, in most cases, association of the negative ion reactant with a single solvent molecule lowers the

SCHEME X

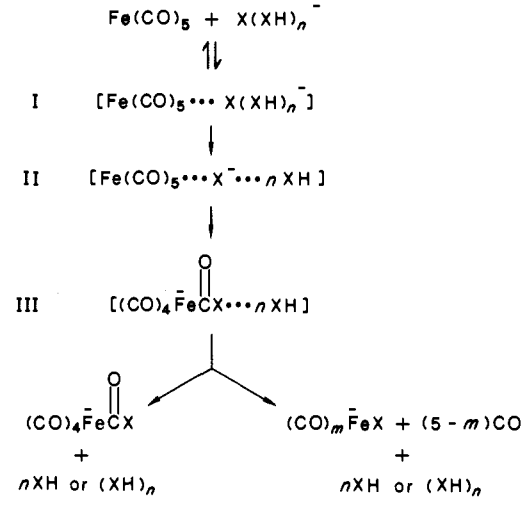

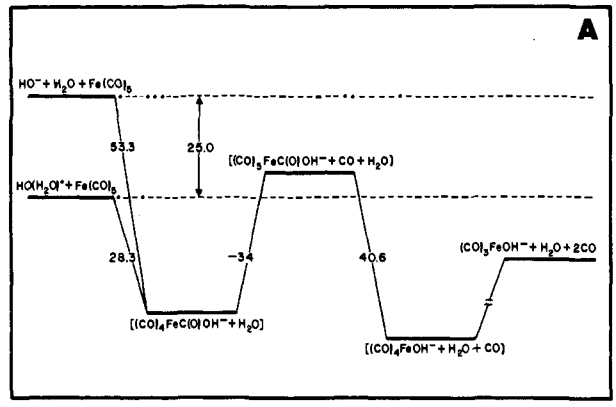

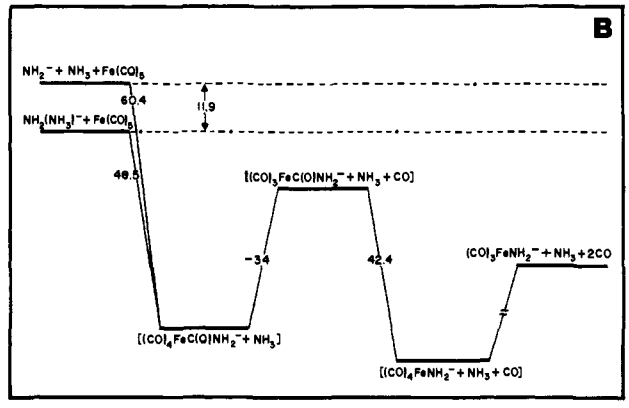

Figure 8. Semiquantitative energy profiles for reactions of OH^-, NH_2^-, and their monosolvated cluster ions with $Fe(CO)_5$. (A) OH^- reacts with bis-decarbonylation while the $OH(H_2O)^-$ ion yields only the hydroxide-transfer product. (B) CO loss accompanies reaction of both NH_2^- and $NH_2(NH_3)^-$ since the total solvation energy in the latter is relatively low. Reprinted with permission from ref 127. Copyright 1986 American Chemical Society.

total energy of the reactants below the estimated barrier for loss of a CO ligand from the tetracarbonyliron acyl ion intermediate (Figure 8). Accordingly, no CO expulsion and only solvent loss result with most all solvated ion reactants except $NH_2(NH_3)^-$, where the initial solvation energy is substantially less.

The particular reactions of $Fe(CO)_5$ with $OH(H_2O)_n^-$ cluster ions (eq 88) are especially interesting since they yield a hydroxycarbonyl complex that was previously believed to be inherently unstable with respect to decarboxylation.[128,129] This ion has been implicated as an

$$HO(H_2O)_n^- + Fe(CO)_5 \xrightarrow{n=0} (CO)_3FeOH^- + 2CO \xrightarrow{n=1-4} (CO)_4FeCOOH^- + nH_2O \quad (88)$$

important intermediate in the formation of $(CO)_4FeH^-$ in aqueous alkaline solutions of $Fe(CO)_5$—a reaction that has been extensively studied as a model for the homogeneously catalyzed water gas shift reaction.[130] Squires and co-workers found that decarboxylation of $(CO)_4FeCOOH^-$ cannot be induced in the gas phase by reaction with neutral amine bases such as NH_3 or NMe_3, despite the fact that CO_2 loss occurs in aqueous solution through a base-catalyzed mechanism.[59,130] Moreover, collisional activation of $(CO)_4FeCOOH^-$ in a flowing afterglow instrument equipped with a triple quadrupole also does not result in decarboxylation, so the metal ion is apparently thermally stable in this respect. An estimate of $\Delta H_f[(CO)_4FeCOOH^-,g] = -259.7 \pm 4.0$ kcal/mol based on the measured energetics for OH^- binding to $Fe(CO)_5$ led to the conclusion that the decarboxylation reaction is indeed exothermic (eq 89), so there must exist a sufficient kinetic energy

$$(CO)_4FeCOOH^- \xrightarrow{\Delta H=-12.7 \text{ kcal/mol}} (CO)_4FeH^- + CO_2 \quad (89)$$

barrier for CO_2 loss to render $(CO)_4FeCOOH^-$ stable and observable in the gas phase on a postmillisecond time scale.

An unusual ion–molecule reaction between H^- and benzenetricarbonylchromium was described recently by Lane and Squires.[90] Two primary products are produced in roughly equal amounts of (eq 90), which cor-

$$H^- + C_6H_6Cr(CO)_3 \rightarrow (C_6H_5)Cr(CO)_3^- + H_2 \rightarrow HCr(CO)_3^- + C_6H_6 \quad (90)$$

respond to proton abstraction and a novel "ligand substitution" of H^- for the η^6-benzene. In order to determine the mechanism for this latter pathway, the reaction with D^- was examined. Deuteride ion was found to yield $HCr(CO)_3^-$ and $DCr(CO)_3^-$ in a 7:1 ratio in the primary product mixture. It was also noted that no H/D exchange occurs in reactions of $HCr(CO)_3^-$ with C_6D_6. A mechanism that is consistent with these observations was proposed (Scheme XI) in which an initial (exo) addition of the nucleophilic D^- to the top face of the metal-complexed benzene ring is accompanied by complete scrambling of hydrogen and deuterium within the energy-rich intermediate. Slower (irreversible) migration of H or D to chromium with accompanying expulsion of neutral benzene produces $HCr(CO)_3^-$ and $DCr(CO)_3^-$ in a near statistical ratio. Another possibility not mentioned in the original paper[90] is for direct attack of D^- at the metal (or CO) to occur every one out of eight encounters, while most of the time exo addition of D^- to the benzene ligand is accompanied by exclusive migration of an endo hydrogen to the metal to form $HCr(CO)_3^-$. In any event, it is clear from this study that nucleophilic addition reactions of $C_6H_6Cr(CO)_3$ in the gas phase can proceed by attack at the benzene ring, just as they do in solution.[131]

SCHEME XI

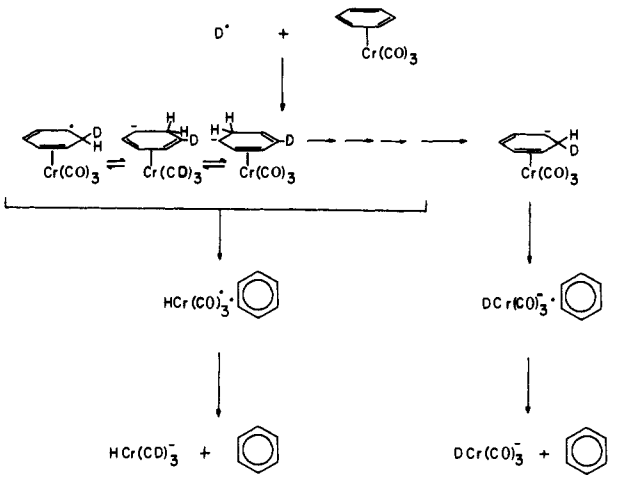

VII. Concluding Remarks

Despite its youth, the field of gas-phase transition-metal negative ion chemistry has already contributed much new information about the intrinsic behavior and physical properties of important types of organometallic and inorganic reactive intermediates. While negative metal ions are typically less reactive kinetically than their positive-ion counterparts, they do exhibit both familiar reactivity patterns and fascinating new behavior that is uniquely their own. Research in this area will undoubtedly continue to grow as the relevance and utility of gas-phase metal ion chemistry becomes more widely appreciated.

Several problem areas were identified in this review as particularly attractive for further development. The reactions of atomic metal anions, particularly those of the second- and third-row elements, should be examined in greater detail under a variety of conditions with a wider range of organic and inorganic substrates. Systematic studies of the properties and reactivity of metal ion complexes with intermediate degrees of coordinative unsaturation are needed in order to evaluate the relationships between the atomic metal ion chemistry that has become so prevalent and the well-documented chemistry of coordination compounds in condensed phases. In this context, specific efforts to generate and characterize metal ions that have been previously proposed as transient intermediates in important catalytic cycles and/or inorganic reactions in solution should be pursued. Cluster chemistry has certainly attracted widespread attention in the past decade, and negative metal ion clusters will no doubt represent an important component in the future development of this field. Finally, in view of the expanding significance of nucleophilic addition and substitution reactions involving organometallic complexes in solution, further studies of their behavior in the gas phase would be useful for evaluating the influence of solvation and ion-pairing.

Acknowledgments. I am grateful to my many colleagues who have kindly supplied numerous preprints of papers concerning their ongoing studies. I especially wish to thank Professor R. N. McDonald for many helpful comments. The work from our laboratory that is described here was supported by grants from the Research Corporation, the National Science Founda-

tion, and the Petroleum Research Fund, administered by the American Chemical Society.

VIII. References

(1) For representative publications, see: Tolbert, M. A.; Beauchamp, J. L. *J. Am. Chem. Soc.* **1986**, *108*, 7509. Jacobson, D. B.; Freiser, B. S. *J. Am. Chem. Soc.* **1983**, *105*, 5197. Aristov, N.; Armentrout, P. B. *J. Am. Chem. Soc.* **1986**, *108*, 1806. Peake, D. A.; Gross, M. L.; Ridge, D. P. *J. Am. Chem. Soc.* **1984**, *106*, 4307. Fredeen, D. A.; Russell, D. H. *J. Am. Chem. Soc.* **1985**, *107*, 3762. Radeki, B. D.; Allison, J. *J. Am. Chem. Soc.* **1984**, *106*, 946. Hanratty, M. A.; Beauchamp, J. L.; Illies, A. J.; Bowers, M. T. *J. Am. Chem. Soc.* **1985**, *107*, 1788. Farrar, J. M.; Sonnenfroh, D. M. *J. Am. Chem. Soc.* **1986**, *108*, 3521. Schulze, C.; Weiske, T.; Schwarz, H. *Chimia* **1986**, *40*, 362. Mandich, M. L.; Steigerwald, M. L.; Reents, W. D. *J. Am. Chem. Soc.* **1986**, *108*, 6197. Magnera, T. F.; David, D. E.; Michl, J. *J. Am. Chem. Soc.* **1987**, *109*, 936. Tonkyn, R.; Weisshaar, J. C. *J. Phys. Chem.* **1986**, *90*, 2305. Mestdagh, H.; Morin, N.; Rolando, L. *Tetrahedron Lett.* **1986**, *27*, 33. Alford, J. M.; Weiss, F. D.; Laaksonen, R. T.; Smalley, R. E. *J. Phys. Chem.* **1986**, *90*, 4480.

(2) Simoes, J. A. M.; Beauchamp, J. L. *Chem. Rev.*, in press.

(3) Forbes, R. A.; Tews, E. C.; Freiser, B. S.; Wise, M. B.; Perone, S. P. *Anal. Chem.* **1986**, *58*, 684.

(4) For reviews, see: Dillard, J. G. *Chem. Rev.* **1973**, *73*, 589. Bowie, J. H. *Mass Spectrom. Rev.* **1984**, *3*, 161.

(5) Parshall, G. *Homogeneous Catalysis*; Wiley: New York, 1982. Gladysz, J. A. *Adv. Organomet. Chem.* **1982**, *20*, 1.

(6) Fischer, E. O.; Maasbol, A. *Angew. Chem., Int. Ed. Engl.* **1964**, *3*, 580. Collman, J. P. *Acc. Chem. Res.* **1975**, *8*, 342. Semmelhack, M. F.; Clark, G. R.; Garcia, J. L.; Harrison, J. J.; Thebtaranonth, Y.; Wulf, W.; Yamashita, A. *Tetrahedron* **1981**, *23*, 3957. Hegedus, L. S. In *The Chemistry of the Carbon–Metal Bond*; Hartley, F. R., Patai, S., Eds.; Wiley: New York, 1982.

(7) Ellis, J. E.; Fjare, K. L.; Hay, T. G. *J. Am. Chem. Soc.* **1981**, *103*, 6100.

(8) Lehman, T. A.; Bursey, M. M. *Ion Cyclotron Resonance Spectroscopy*; Wiley-Interscience: New York, 1976.

(9) Wronka, J.; Ridge, D. P. *Rev. Sci. Instrum.* **1982**, *53*, 107 and references cited therein.

(10) McIver, R. T.; Hunter, R. L.; Ledford, E. B.; Locke, M. J.; Francl, T. J. *Int. J. Mass Spectrom. Ion Phys.* **1981**, *39*, 65.

(11) Comisarov, M. B.; Marshall, A. G. *Chem. Phys. Lett.* **1974**, *25*, 282. For a recent review of the technique, see: Laude, D. A.; Johlman, C. L.; Brown, R. S.; Weil, D. A.; Wilkins, C. L. *Mass Spectrom. Rev.* **1986**, *5*, 107.

(12) Carlin, T. J.; Freiser, B. S. *Anal. Chem.* **1983**, *55*, 571.

(13) Cody, R. B.; Burnier, R. C.; Freiser, B. S. *Anal. Chem.* **1982**, *54*, 96.

(14) Froelicher, S. W.; Freiser, B. S.; Squires, R. R. *J. Am. Chem. Soc.* **1986**, *108*, 2853. Froelicher, S. W.; Freiser, B. S.; Squires, R. R. *J. Am. Chem. Soc.* **1984**, *106*, 6863. Jacobson, D. B.; Freiser, B. S. *J. Am. Chem. Soc.* **1985**, *107*, 1581.

(15) Cody, R. B.; Burnier, R. C.; Reents, W. D.; Carlin, T. J.; McCrery, D. A.; Lengal, R. K.; Freiser, B. S. *Int. J. Mass Spectrom. Ion Phys.* **1980**, *33*, 37. Bondybey, V. E.; Reents, W. D.; Mandich, M. L. *J. Chem. Phys.*, in press.

(16) Castro, M. E.; Russell, D. H.; Amster, I. J.; McLafferty, F. W. *Anal. Chem.* **1986**, *58*, 483.

(17) Huntress, W. T.; Simms, W. T. *Rev. Sci. Instrum.* **1973**, *44*, 1274.

(18) Ferguson, E. E.; Fehsenfeld, F. C.; Schmeltekopf, A. L. *Adv. At. Mol. Phys.* **1969**, *5*, 1.

(19) Smith, D.; Adams, N. G. In *Gas Phase Ion Chemistry*; Bowers, M. T., Ed.; Academic: New York, 1979; Chapter 1.

(20) Bohme, D. K.; Dunkin, D. B.; Fehsenfeld, F. C.; Ferguson, E. E. *J. Chem. Phys.* **1969**, *51*, 863.

(21) Albritton, D. L. *At. Data Nucl. Data Tables* **1978**, *22*, 1.

(22) Goldan, P. D.; Schmeltekopf, A. L.; Fehsenfeld, F. C.; Schiff, H. I.; Ferguson, E. E. *J. Chem. Phys.* **1966**, *44*, 4095. Damrauer, R.; DePuy, C. H.; Davidson, I. M. T.; Hughes, K. J. *Organometallics* **1986**, *5*, 2050, 2054.

(23) *The Characterization of High-Temperature Vapors*; Margrave, J. L., Ed.; Wiley: New York, 1967.

(24) Sidorov, L. N.; Zhuravleva, L. V.; Sorokin, I. D. *Mass Spectrom. Rev.* **1986**, 573. Sidorov, L. N.; Nikitin, M. I.; Skokan, E. V.; Sorokin, I. D. *Int. J. Mass Spectrom. Ion Phys.* **1980**, *35*, 203.

(25) Sidorov, L. N.; Sorokin, I. D.; Nikitin, M. I.; Skokan, E. V. *Int. J. Mass Spectrom. Ion Phys.* **1981**, *39*, 311.

(26) Chilingarov, N. S.; Korobov, M. V.; Sidorov, L. N.; Mit'kin, V. N.; Shipachev, V. A.; Zemskov, S. V. *J. Chem. Thermodyn.* **1984**, *16*, 965.

(27) Nikitin, M. I.; Igolkina, N. A.; Borshchevskii, A. Y.; Sidorov, L. N. *Dokl. Akad. Nauk. SSSR* **1983**, *272*, 1165. Rudny, E. B.; Sidorov, L. N.; Kuligina, L. A.; Semenov, G. A. *Int. J. Mass Spectrom. Ion Processes* **1985**, *64*, 95.

(28) Hotop, H.; Lineberger, W. C. *J. Phys. Chem. Ref. Data* **1985**, *14*, 731. Feigerle, C. S.; Corderman, R. R.; Bobashev, S. V.; Lineberger, W. C. *J. Chem. Phys.* **1981**, *74*, 1580.

(29) Middleton, R. *Nucl. Instrum. Methods* **1977**, *144*, 373.

(30) Sallans, L.; Lane, K. R.; Squires, R. R.; Freiser, B. S. *J. Am. Chem. Soc.* **1983**, *105*, 6352.

(31) Sallans, L.; Lane, K. R.; Squires, R. R.; Freiser, B. S. *J. Am. Chem. Soc.* **1985**, *107*, 4379.

(32) Allison, J.; Freas, R. B.; Ridge, D. P. *J. Am. Chem. Soc.* **1979**, *101*, 1332.

(33) Moore, C. E. *Atomic Energy Levels*; National Bureau of Standards: Washington, DC, 1971.

(34) Tonkyn, R.; Weisshaar, J. C. *J. Phys. Chem.* **1986**, *90*, 2305.

(35) Armentrout, P. B.; Halle, L. F.; Beauchamp, J. L. *J. Am. Chem. Soc.* **1981**, *103*, 6501. Elkind, J. L.; Armentrout, P. B. *Inorg. Chem.* **1986**, *25*, 1078.

(36) Squires, R. R. *J. Am. Chem. Soc.* **1985**, *107*, 4385.

(37) Bartmess, J. E.; McIver, R. T., Jr. In *Gas Phase Ion Chemistry*; Bowers, M. T., Ed.; Academic: New York, 1979; Chapter 11. Bartmess, J. E. *J. Phys. Chem. Ref. Data*, in press.

(38) Pearson, R. G. *Chem. Rev.* **1985**, *85*, 4.

(39) Additional support for the validity of this correlation may be found in: Tolbert, M. A.; Beauchamp, J. L. *J. Phys. Chem.* **1986**, *90*, 5015.

(40) Weil, D. A.; Wilkins, C. L. *J. Am. Chem. Soc.* **1985**, *107*, 7316.

(41) Gregor, I. K.; Guilhaus, M. *Mass Spectrom. Rev.* **1984**, *3*, 39.

(42) Winters, R. E.; Kiser, R. W. *J. Chem. Phys.* **1966**, *44*, 1964. George, P. M.; Beauchamp, J. L. *J. Chem. Phys.* **1982**, *76*, 2959.

(43) Giordan, J. C.; Moore, J. H.; Tossell, J. A. In *Resonances in Electron–Molecule Scattering, van der Waals Complexes, and Reactive Chemical Dynamics*; Truhlar, D. G., Ed.; American Chemical Society: Washington, DC, 1984.

(44) Compton, R. N.; Stockdale, J. A. D. *Int. J. Mass Spectrom. Ion Phys.* **1976**, *22*, 47.

(45) McDonald, R. N.; Chowdhury, A. K.; Schell, P. L. *J. Am. Chem. Soc.* **1984**, *106*, 6095.

(46) Meckstroth, W. K.; Ridge, D. P. *J. Am. Chem. Soc.* **1985**, *107*, 2281.

(47) Blake, M. R.; Garnett, J. L.; Gregor, I. K.; Wild, S. B. *J. Organomet. Chem.* **1979**, *178*, C37.

(48) Blake, M. R.; Garnett, J. L.; Gregor, I. K.; Wild, S. B. *Chem. Commun.* **1979**, 496.

(49) Murr, N. E.; Payne, J. D. *Chem. Commun.* **1985**, 162.

(50) Krusic, P. L.; San Filippo, J. *J. Am. Chem. Soc.* **1982**, *104*, 2654.

(51) Engelking, P. C.; Lineberger, W. C. *J. Am. Chem. Soc.* **1979**, *101*, 5569.

(52) Stevens, A. E.; Feigerle, C. S.; Lineberger, W. C. *J. Am. Chem. Soc.* **1982**, *104*, 5026.

(53) Leopold, D. G.; Murray, K. K.; Lineberger, W. C., private communication of unpublished results.

(54) Elian, M.; Hoffman, R. *Inorg. Chem.* **1975**, *14*, 1058.

(55) Dunbar, R. C.; Hutchinson, B. B. *J. Am. Chem. Soc.* **1974**, *96*, 3816.

(56) Pignataro, S.; Foffani, A.; Grasso, F.; Cantone, B. *Z. Phys. Chem. (Munich)* **1965**, *47*, 106.

(57) Mead, R. D.; Stevens, A. E.; Lineberger, W. C. In *Gas Phase Ion Chemistry*; Bowers, M. T., Ed.; Academic: New York, 1984; Chapter 22.

(58) Engelking, P. C.; Lineberger, W. C. *J. Chem. Phys.* **1977**, *66*, 5054.

(59) Murad, E. *J. Chem. Phys.* **1980**, *73*, 1381.

(60) McDonald, R. N.; Schell, P. L.; McGhee, W. D. *Organometallics* **1984**, *3*, 182.

(61) Pearson, R. G.; Mauerman, H. *J. Am. Chem. Soc.* **1982**, *104*, 500.

(62) Stevens, A. E.; Feigerle, C. S.; Lineberger, W. C. *J. Chem. Phys.* **1983**, *78*, 5420.

(63) Lane, K. R.; Sallans, L.; Squires, R. R. *J. Am. Chem. Soc.* **1985**, *107*, 5369.

(64) Flesch, G. D.; White, R. M.; Svec, H. J. *Int. J. Mass Spectrom. Ion Phys.* **1969**, *3*, 339.

(65) Corderman, R. R.; Beauchamp, J. L. *J. Am. Chem. Soc.* **1976**, *98*, 3998. Jones, R. W.; Staley, R. H. *J. Am. Chem. Soc.* **1982**, *104*, 2296. Weddle, G. H.; Allison, J.; Ridge, D. P. *J. Am. Chem. Soc.* **1977**, *99*, 105.

(66) Atwood, J. D. *Inorganic and Organometallic Reaction Mechanisms*; Brooks-Cole: Monterey, CA, 1985.

(67) Sieck, L. W.; Mautner, M. *J. Phys. Chem.* **1982**, *86*, 3646 and references therein.

(68) Corderman, R. R.; Beauchamp, J. L. *Inorg. Chem.* **1976**, *15*, 665.

(69) Corderman, R. R.; Beauchamp, J. L. *Inorg. Chem.* 1977, *16*, 3135.
(70) Wang, D.; Squires, R. R. *Organometallics*, in press.
(71) Cotton, F. A.; Wilkinson, G. *Advanced Inorganic Chemistry*, 3rd ed.; Wiley: New York, 1972.
(72) McDonald, R. N.; Chowdhury, A. K. *Organometallics* 1986, *5*, 1187.
(73) Lane, K. R.; Sallans, L.; Squires, R. R. *J. Am. Chem. Soc.* 1984, *106*, 2719.
(74) Wang, D.; Lane, K. R.; Squires, R. R., unpublished results.
(75) Scott, P. R.; Richards, W. G. In *Molecular Spectroscopy*; The Chemical Society: London, 1976. Chem. Soc. Spec. Per. Reports; Cheetham, G. J.; Barrow, R. F. *Adv. High Temp. Chem.* 1967, *1*, 7.
(76) Lewis, K. E.; Golden, D. M.; Smith, G. P. *J. Am. Chem. Soc.* 1984, *106*, 3905.
(77) Almond, M. J.; Crayston, J. A.; Downs, A. J.; Poliakoff, M.; Turner, J. J. *Inorg. Chem.* 1986, *25*, 19.
(78) For reviews see: Collman, J. P.; Hegedus, L. S.; Norton, J. R.; Finke, R. G. In *Principles and Applications of Organotransition Metal Chemistry*; University Science: Mill Valley, CA, 1987. Collman, J. P.; Roper, W. R. *Adv. Organomet. Chem.* 1968, *1*, 136. Vaska, L. *Acc. Chem. Res.* 1968, *1*, 335. Kemmitt, R. D. W.; Smith, M. A. R. *Inorg. React. Mech.* 1976, *4*, 3119.
(79) Low, J. J.; Goddard, W. A. *J. Am. Chem. Soc.* 1986, *108*, 6115 and references cited therein.
(80) Allison, J.; Ridge, D. P. *J. Am. Chem. Soc.* 1976, *98*, 7445.
(81) Allison, J. *Prog. Inorg. Chem.* 1986, 34.
(82) McDonald, R. N.; Schell, P. L.; Chowdhury, A. K. *J. Am. Chem. Soc.* 1985, *107*, 5578.
(83) McDonald, R. N.; Chowdhury, A. K.; Jones, M. T. *J. Am. Chem. Soc.* 1986, *108*, 3105.
(84) McDonald, R. N.; Jones, M. T., private communication of unpublished results.
(85) McDonald, R. N.; Jones, M. T. *Organometallics*, in press.
(86) McDonald, R. N.; Jones, M. T. *J. Am. Chem. Soc.* 1986, *108*, 8097.
(87) (a) McElvany, S. W.; Allison, J. *Organometallics* 1986, *5*, 416. (b) McElvany, S. W.; Allison, J. *Organometallics* 1986, *5*, 1219.
(88) Blumer, D. J.; Barnett, K. W.; Brown, T. L. *J. Organomet. Chem.* 1973, *173*, 71.
(89) McDonald, R. N.; Chowdhury, A. K.; Schell, P. L. *Organometallics* 1984, *3*, 644.
(90) Lane, K. R.; Squires, R. R. *J. Am. Chem. Soc.* 1985, *107*, 6403.
(91) Thompson, M. E.; Baxter, S. M.; Bulls, A. R.; Burger, B. J.; Nolan, M. C.; Santarisiero, B. D.; Schaefer, W. P.; Bercaw, J. E. *J. Am. Chem. Soc.* 1987, *109*, 203.
(92) Doherty, N. M.; Bercaw, J. E. *J. Am. Chem. Soc.* 1985, *107*, 2670.
(93) Faller, J. W.; Felkin, H. *Organometallics* 1985, *4*, 1488. Stoutland, P. O.; Bergman, R. G. *J. Am. Chem. Soc.* 1985, *107*, 4581. Fujimoto, H.; Yamasaki, T.; Mizutani, H.; Koga, N. *J. Am. Chem. Soc.* 1985, *107*, 6157. Kafafi, Z. H.; Hauge, R. H.; Margrave, J. L. *J. Am. Chem. Soc.* 1985, *107*, 7550.
(94) Crabtree, R. N. *Chem. Rev.* 1985, *85*, 245.
(95) McMillen, D. F.; Golden, D. M. *Annu. Rev. Phys. Chem.* 1982, *33*, 493.
(96) Dunbar, R. C.; Ennever, J. F.; Fackler, J. P. *Inorg. Chem.* 1973, *12*, 2734.
(97) Richardson, J. H.; Stephenson, L. M.; Brauman, J. I. *J. Am. Chem. Soc.* 1974, *96*, 3671.
(98) Foster, M. S.; Beauchamp, J. L. *J. Am. Chem. Soc.* 1975, *97*, 4808.
(99) Schore, N. E.; Ilenda, C. S.; Bergman, R. G. *J. Am. Chem. Soc.* 1977, *99*, 1781.
(100) Schore, N. E.; Ilenda, C. S.; Bergman, R. G. *J. Am. Chem. Soc.* 1976, *98*, 256.
(101) Wronka, J.; Ridge, D. P. *Int. J. Mass Spectrom. Ion Phys.* 1982, *43*, 23.
(102) Wronka, J.; Ridge, D. P. *J. Am. Chem. Soc.* 1984, *106*, 67.
(103) Sallans, L.; Lane, K. R.; Squires, R. R.; Freiser, B. S., unpublished results. Cf.: Sallans, L. Ph.D. Thesis, Purdue University, W. Lafayette, IN, 1985.
(104) Leopold, D. G.; Miller, T. M.; Lineberger, W. C. *J. Am. Chem. Soc.* 1986, *108*, 178. Leopold, D. G.; Lineberger, W. C. *J. Chem. Phys.* 1986, *85*, 51. Leopold, D. G.; Ho, J.; Lineberger, W. C. *J. Chem. Phys.* 1987, *86*, 1715. Zheng, L. S.; Karner, C. M.; Brucat, P. J.; Yang, S. H.; Pettiette, C. L.; Craycraft, M. J.; Smalley, R. E. *J. Chem. Phys.* 1986, *85*, 1681.
(105) Olmstead, W. N.; Brauman, J. I. *J. Am. Chem. Soc.* 1977, *99*, 4219. Asubiojo, O. I.; Brauman, J. I. *J. Am. Chem. Soc.* 1979, *101*, 3715. Pellerite, M. J.; Brauman, J. I. *J. Am. Chem. Soc.* 1980, *102*, 5993. Caldwell, G.; Magnera, T. F.; Kebarle, P. *J. Am. Chem. Soc.* 1984, *106*, 959.
(106) Foster, M. S.; Beauchamp, J. L. *J. Am. Chem. Soc.* 1971, *93*, 4924.
(107) Kowaleski, R. M.; Rheingold, A. L.; Trogler, W. C.; Basolo, F. *J. Am. Chem. Soc.* 1986, *108*, 2460 and references cited therein.
(108) Kahn, S. D.; Hehre, W. J.; Bartmess, J. E.; Caldwell, G. *Organometallics* 1984, *3*, 1740.
(109) Nikitin, M. I.; Sorokin, I. D.; Skokan, E. V.; Sidorov, L. N. *Zh. Fiz. Khim.* 1980, *54*, 1336.
(110) Sidorov, L. N.; Skokan, E. V.; Nikitin, M. I.; Sorokin, I. D. *Int. J. Mass Spectrom. Ion Phys.* 1980, *35*, 215.
(111) Nikitin, M. I.; Sidorov, L. N.; Skokan, E. V.; Sorokin, I. D. *Zh. Fiz. Khim* 1981, *55*, 1944.
(112) Sorokin, I. D.; Sidorov, L. N.; Nikitin, M. I.; Skokan, E. V. *Int. J. Mass Spectrom. Ion Phys.* 1981, *41*, 45.
(113) Skokan, E. V.; Nikitin, M. I.; Sorokin, I. D.; Gusarov, A. V.; Sidorov, L. N. *Zh. Fiz. Khim.* 1981, *55*, 1871.
(114) Skokan, E. V.; Sorokin, I. D.; Sidorov, L. N.; Nikitin, M. I. *Int. J. Mass Spectrom. Ion Phys.* 1982, *43*, 309.
(115) Korobov, M. V.; Chilingarov, N. S.; Igolkina, N. A.; Nikitin, M. I.; Sidorov, L. N. *Zh. Fiz. Khim.* 1984, *58*, 2250.
(116) Igolkina, N. A.; Nikitin, M. I.; Sidorov, L. N.; Petrov, S. V. *Zh. Fiz. Khim.* 1984, *58*, 2342.
(117) Chilingarov, N. S.; Korobov, M. V.; Rudometkin, S. V.; Alikhanyan, A. S.; Sidorov, L. N. *Int. J. Mass Spectrom. Ion Processes* 1986, *69*, 175.
(118) Borschevski, A. Ya.; Sidorov, L. N.; Boltalina, O. V. *Dokl. Akad. Nauk SSSR* 1985, *285*, 377.
(119) Igolkina, N. A.; Nikitin, M. I.; Boltalina, O. V.; Sidorov, L. N. *High Temp. Sci.* 1986, *21*, 111.
(120) Nikitin, M. I.; Sidorov, L. N.; Korobov, M. V. *Int. J. Mass Spectrom. Ion Phys.* 1981, *37*, 13.
(121) George, P. M.; Beauchamp, J. L. *Chem. Phys.* 1979, *36*, 345.
(122) Morgan, R. P.; Gilchrist, C. A.; Jennings, K. R.; Gregor, I. K. *Int. J. Mass Spectrom. Ion Phys.* 1983, *46*, 309.
(123) Dillow, G. W.; Gregor, I. K. *Inorg. Chim. Acta* 1984, *86*, 267.
(124) Turco, A.; Morvillo, S.; Bettori, V.; Traldi, P. *Inorg. Chem.* 1985, *24*, 1123.
(125) Lane, K. R.; Sallans, L.; Squires, R. R. *J. Am. Chem. Soc.* 1986, *108*, 4368.
(126) Lane, K. R.; Sallans, L.; Squires, R. R. *Organometallics* 1985, *3*, 408.
(127) Lane, K. R.; Squires, R. R. *J. Am. Chem. Soc.* 1986, *108*, 7187.
(128) Lane, K. R.; Sallans, L.; Squires, R. R. *Inorg. Chem.* 1984, *23*, 1999.
(129) Lane, K. R.; Lee, R. E.; Sallans, L.; Squires, R. R. *J. Am. Chem. Soc.* 1984, *106*, 5767.
(130) Trautman, R. J.; Gross, D. C.; Ford, P. C. *J. Am. Chem. Soc.* 1985, *107*, 2355 and references therein.
(131) Kundig, E. P.; Desobry, V.; Simmons, D. P. *J. Am. Chem. Soc.* 1983, *105*, 6962 and references therein.